CONFIDENTIAL

R-5381

59 p

X64 12839

Code 2D

CLASSIFICATION CHANGE

TO - UNCLASSIFIED

By authority of E.O. 11652

Changed by L. Shirley Date 12-20-73

NASA CR 55891

Interim Report

AERODYNAMIC NOZZLE STUDY
VOLUME I SUMMARY

(UNCLASSIFIED TITLE)

ROCKETDYNE
A DIVISION OF NORTH AMERICAN AVIATION, INC.
6633 CANOGA AVENUE, CANOGA PARK, CALIFORNIA

1980994

ROCKETDYNE, Canoga Park, Calif.
A DIVISION OF NORTH AMERICAN AVIATION, INC

9

~~CONFIDENTIAL~~

(NASA CR R-5381) (Unclassified Title)

Volume I - Summary

Interim Report, 1 Jun. 1962 - 1 Sep. 1963

Aerodynamic Nozzle Study. VOLUME SUMMA

October 1, 1963

Prepared for

NATIONAL AERONAUTICS AND SPACE ADMINISTRATION

NASA HEADQUARTERS

Mr. H. Burlage,

MSFC

Mr. K. Chandler, and
Mr. J. McCarty, 1 Oct. 1963

(NASA contract NAS8-2654)

"Available to U.S. Government Agencies and U.S. Government Contractors Only"

Prepared By

ADVANCED SYSTEMS SECTION

A. Martinez

A. Martinez
Responsible Engineer

APPROVED BY:

S. F. Iacobellis

S. F. Iacobellis
Section Chief
Advanced Systems

~~DOWNGRADED AT 3 YEAR INTERVALS~~
~~DECLASSIFIED AFTER 12 YEARS~~
~~DOD DIR 5200.10~~

~~THIS MATERIAL CONTAINS INFORMATION AFFECTING THE NATIONAL DEFENSE OF THE UNITED STATES WITHIN THE MEANING OF THE ESPIONAGE LAWS, TITLE 18 U. S. C., SECTIONS 793 AND 794. ITS TRANSMISSION OR THE REVELATION OF ITS CONTENTS IN ANY MANNER TO AN UNAUTHORIZED PERSON IS PROHIBITED BY~~

~~CONFIDENTIAL~~

FORM 608-B-1 (LEDGER) REV. 1-58

FOREWORD

This report describes studies of the aerodynamic nozzle concept conducted from June 1, 1962 to September 1, 1963, under National Aeronautics and Space Administration Contract NAS 8-2654.

ABSTRACT

12839 A

The results of analytical and experimental studies conducted to evaluate the feasibility of the aerodynamic nozzle concept are presented. The objective of the analytical studies was prediction of performance by a solution of the aerodynamic nozzle flow field. Wind tunnel tests were made to evaluate aerodynamic nozzle efficiency and the effect of various nozzle geometric parameters and secondary flow on nozzle performance. Hot-firing tests were conducted to demonstrate the feasibility of concentric tube and aerodynamic spike nozzles, and to verify cold-flow nozzle performance and secondary-pressure trends. Cnf. Author

TABLE OF CONTENTS

ILLUSTRATIONS

TABLES

INTRODUCTION

During the recent years, various new thrust chamber configurations have been conceived. The ultimate objective of these advanced concepts has been to provide efficient expansion in a structure which is simple, light in weight, short in length, and relatively simple to cool. One attempt to satisfy these objectives has been the annular nozzle.

Much of the recent work on annular nozzles has evaluated the effect of various nozzle design parameters, most notably length. Data relative to the variation of length and its affect on annular nozzle performance have recently been generated. The performance of shortened plug configurations has been high. Very short plugs have maintained efficiencies over 95 percent. Even the performance of zero-length plugs is sufficient to warrant consideration of this configuration for certain applications.

Another promising approach to minimum nozzle length currently under evaluation is referred to as the aerodynamic nozzle concept. Here a boundary is formed by the interaction of two gas streams which is analogous to a divergent nozzle contour. Originally, this concept was envisioned as a replacement for the divergent portion of the bell and conical nozzles used in current engines. This version of the aerodynamic nozzle was referred to as the concentric tube model. High-pressure primary gases are exhausted from a central tube surrounded by low-pressure secondary gases. By this action an interface between the flows is formed which might be referred to as a nozzle. The thrust contribution normally attributed to a nozzle is obtained by the pressure of the secondary gases acting over the base.

The same concept was readily envisioned as a method of shortening the spike (plug) contour. This version is the aerodynamic spike. In the aerodynamic spike, high-pressure primary gases are exhausted from an annular-type combustion chamber with low-pressure gases coming out of the central portion. Outwardly, this configuration looks much like the zero-length plug, the difference being that aerodynamic spike secondary flow is used to improve the base pressure created by the primary gases. This improved base pressure results from the interaction of the two gas streams.

Performance of the aerodynamic nozzle is a function of various nozzle geometric parameters, of the amount of secondary flow, and of the manner in which this secondary flow is introduced. Investigation of these parameters for the concentric tube aerodynamic nozzle configuration was conducted, to a certain extent, under a company-sponsored study. Further study to prove the feasibility of the aerodynamic spike concept and to extend the range of experimental data for the concentric tube aerodynamic nozzle was required. In particular, further study would ek to prove the feasibility of the aerodynamic spike nozzle by monstrating its capability of producing higher-than-sonic nozzle rformance and the potential of delivering performance comparable to nventional nozzle performance through proper selection of important ozzle parameters. For this demonstration, a complete evaluation of ne parameters that affect nozzle performance and the degree to which ney affect such performance was required.

ONCEPT DESCRIPTION

his concept can be illustrated most simply by using the concentric-ube model in Fig. 1 as a reference. The boundary between the rimary and secondary gas streams forms the aerodynamic expansion urface. The hot primary gas stream is prevented from contacting the xternal structural surface of the stovepipe shroud by secondary gas low. As a result of the growth in cross-sectional area of the primary stream, the secondary stream is accelerated and approaches sonic velocity at the exit. Thrust of the system consists of contributions from stabilized upstream pressures on the primary and secondary nozzle surfaces. Preliminary tests indicated that the concentric tube nozzle would give good performance with short nozzle lengths, thus reducing nozzle weight and interstage structure length and weight.

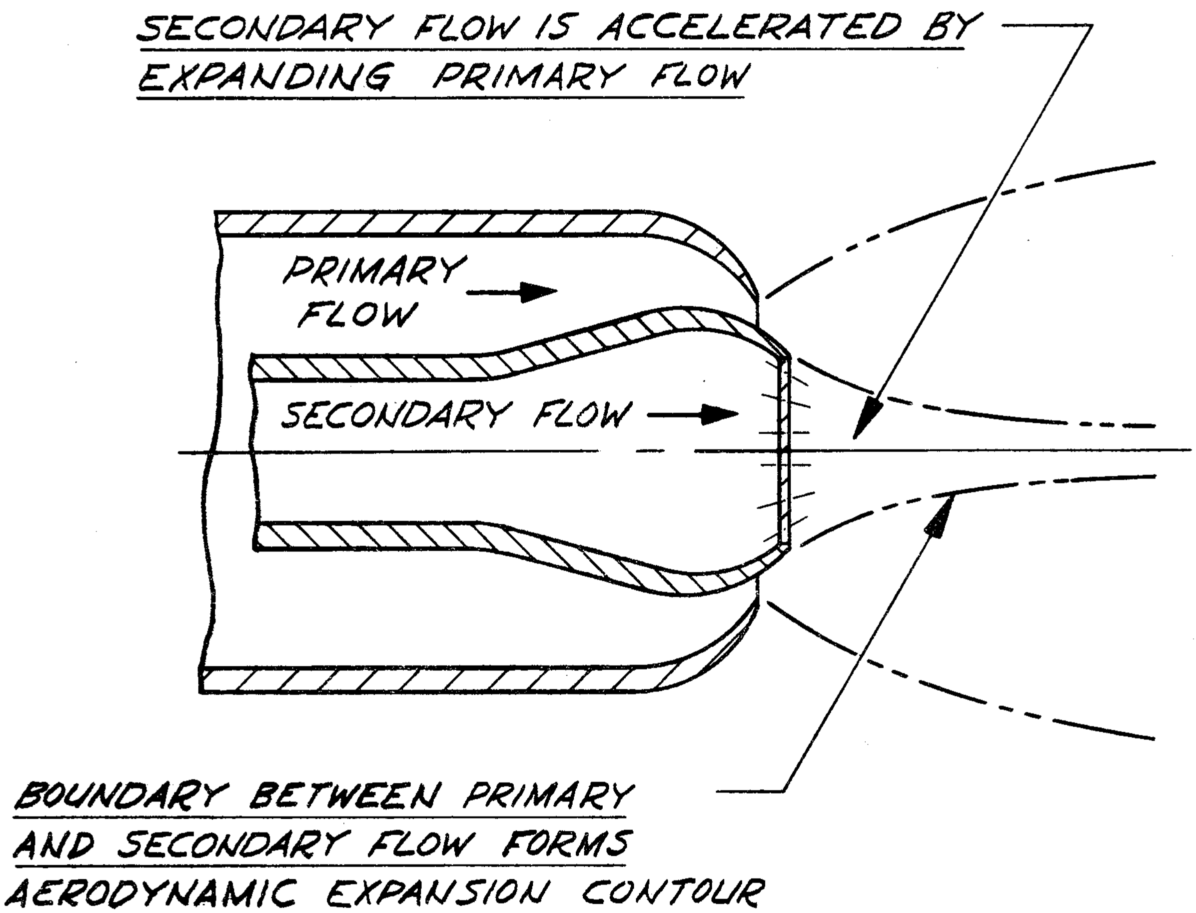

AERODYNAMIC SPIKE NOZZLE CONCEPT
FIGURE 2

FIGURE 2

CONFIDENTIAL

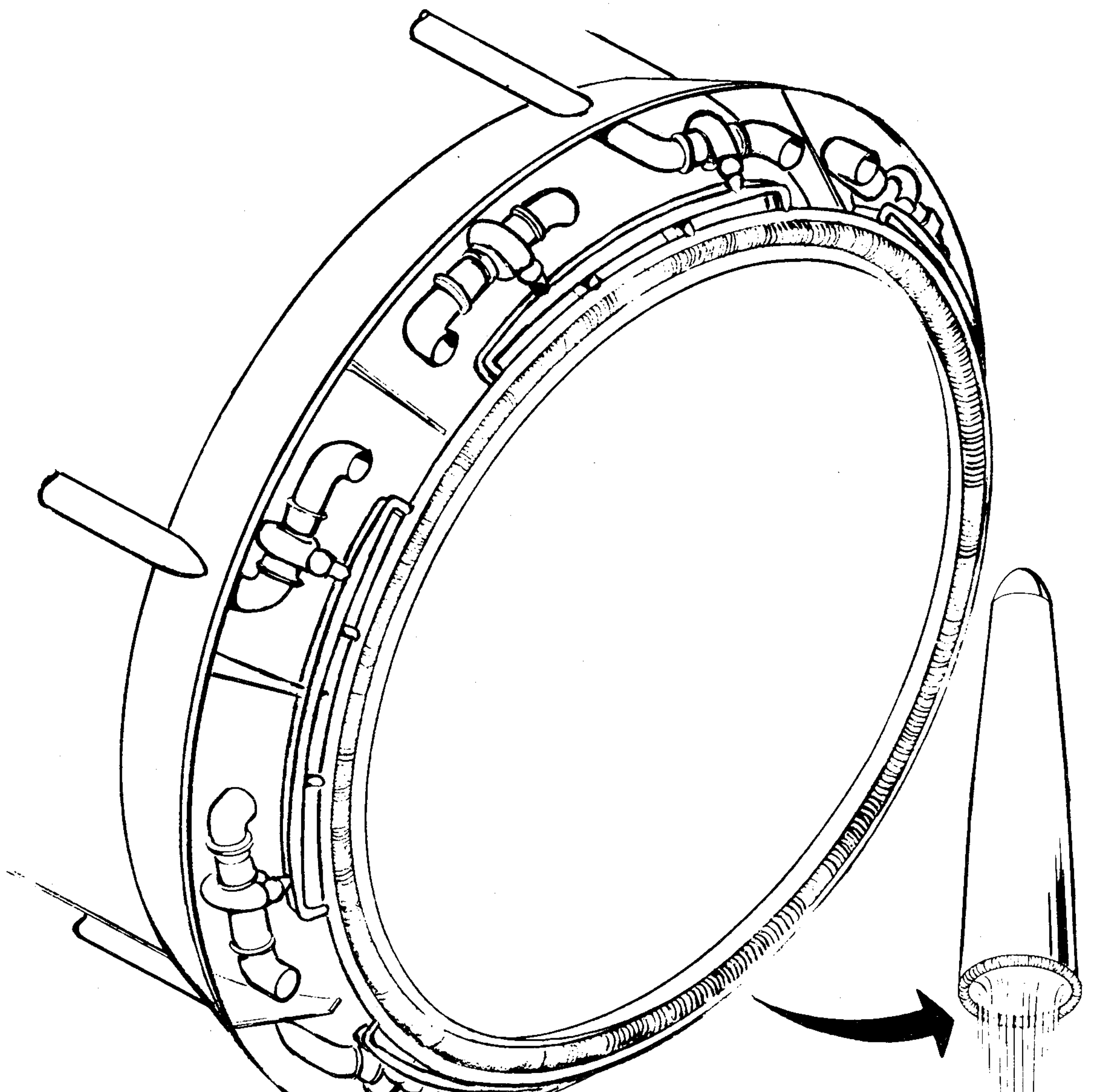

Figure 3. Engine-Missile Integration, Aerodynamic Spike Concept

ANALYTICAL STUDIES

Knowledge of nozzle performance and its variation with parameters such as nozzle geometry, gas composition, and external slip-stream flow is essential in the application of a nozzle concept to specific missions. Therefore, the initial goal of the analytical studies was to develop a method of predicting performance of aerodynamic nozzle configurations. For both aerodynamic nozzles, this problem is similar in many ways to the problem of determining efficiency of aircraft ejectors. The flow field of the aircraft ejector has been the object of extensive study for many years; however, there is still a great deal to be learned of the complex interaction of its primary and secondary flows.

A common feature of aircraft ejectors and of the two aerodynamic nozzle configurations is the interaction between a supersonic primary flow and a subsonic secondary flow. These boundary conditions are illustrated for the aerodynamic nozzle concept in Figs. 4A and 4B. In the concentric tube nozzle, the expanding primary stream is surrounded by the secondary subsonic jet boundary; while in the aerodynamic spike nozzle, the expanding primary stream surrounds the secondary subsonic jet boundary. The primary stream in the aerodynamic spike may be surrounded by either slipstream or still ambient conditions.

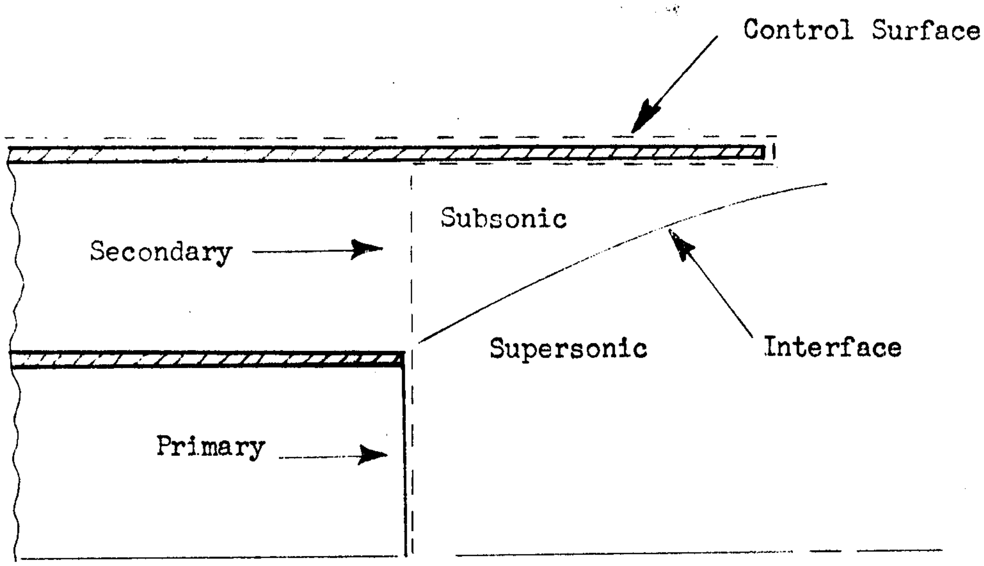

A. Concentric-Tube Configuration

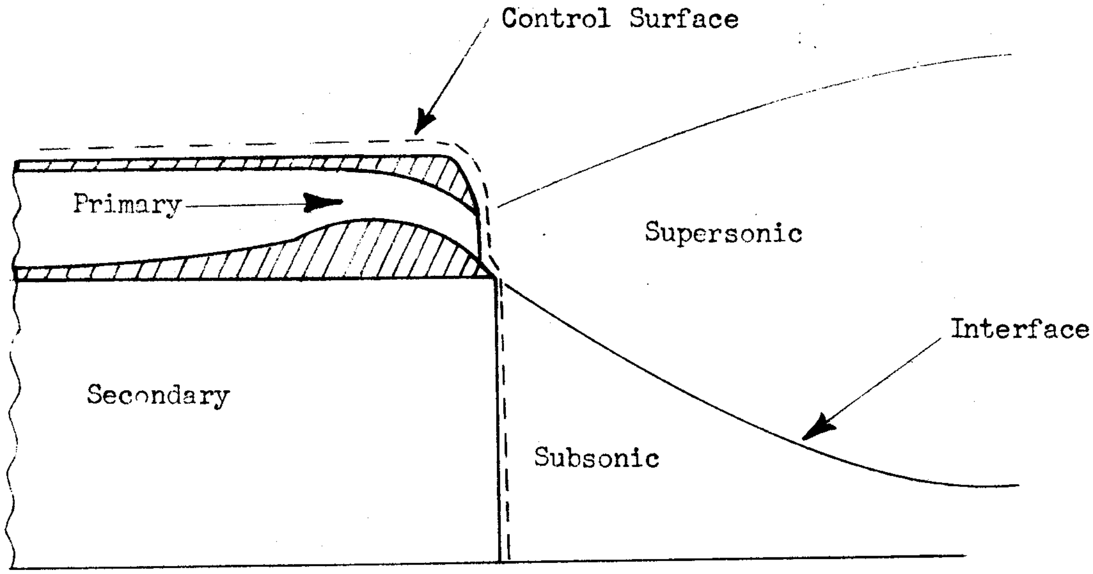

B. Aerodynamic Spike Configuration

ILLUSTRATION OF THEORETICAL MODELS

Figure 4

In the aerodynamic spike nozzle, the primary gases accelerate the centercore of subsonic gases; consequently, the secondary gases expand. Expansion of the primary and secondary gases produces a reaction force or thrust which is transmitted to the nozzle structure. Evaluation of this thrust is possible if the properties of the flow are known along a control surface, such as shown in Fig. 4B, which includes both primary and secondary flow regimes. In other words, both primary and secondary flow fields must be defined at the control surface.

In the concentric tube aerodynamic nozzle, the primary stream flows inside a tubular enclosure surrounded at its periphery by a subsonic secondary flow. As illustrated in the Fig. 4 A, the primary and secondary streams expand along a common boundary or interface. As a result of the expansion of the gases, a thrust is developed which can be evaluated if the flow properties along a control surface such as shown in the figure are known.

During the initial phase of the aerodynamic nozzle study, an evaluation was made of the problems associated with the solution of the flow fields, and the means that are available for their solution. It was established that a purely one-dimensional approach would be inadequate and that a more general approach would be required.

For the concentric tube, an iterative solution to the boundary between the primary and secondary flow fields was recommended. The primary flow field is determined by the axially-symmetric method of characteristics while the secondary flow field is assumed one-dimensional in nature. Initially, a set of input conditions defining the primary and secondary flow properties is assumed. The boundary between secondary and primary flow may then be established and flow properties at a flow cross section just outside the nozzle compared to flow properties demanded by mixing theory. If these sets of flow properties disagree, another set of input conditions is assumed and the process repeated until agreement is effected. This general solution requires the use of a suitable mixing theory and assumption of one-dimensional flow in the secondary. These requirements may be fulfilled for most concentric tube nozzle configurations. However, the method would fail for cases with sharp curvatures of the interface between primary and secondary flows. This would make the assumption of one-dimensional flow in the secondary invalid.

A general approach to the solution of the flow fields in the aerodynamic spike nozzle similar to the one outlined above for the concentric tube nozzle is not possible in all cases. Because of the converging nature of the primary flow in the cases of interest, the boundary between primary and secondary flows have very sharp curvatures so that one-dimensionality of flow in the secondary is not a valid assumption. A more general theoretical approach would necessitate a better understanding of the mixing mechanism, which is at present not amenable to theoretical formulation. Until reliable base pressure and mixing theories can be developed, aerodynamic spike nozzle performance prediction will rely heavily on empirical information in the form of secondary flow pressures (base pressures) derived from wind tunnel tests under the present contract, or obtained from a survey of literature on related base pressure and ejector theory and experiment. With the knowledge of the secondary pressures, solution of the flow field in the region of interaction of primary and secondary flow, for the purpose of thrust prediction, is not necessary. Thrust may be derived from knowledge of base pressures and the solution of that portion of the primary flow field in the immediate vicinity of the primary-flow physical surfaces. This flow field yields to an axially-symmetric method of characteristics.

WIND TUNNEL STUDIES

Previous wind tunnel work performed at Rocketdyne had demonstrated the feasibility of the concentric tube aerodynamic nozzle. It was the main goal of the wind tunnel program of this study to evaluate the feasibility of the aerodynamic spike nozzle by examining its capability of producing higher-than-sonic nozzle performance, and the potential of performance improvement through optimization of appropriate parameters. To demonstrate these capabilities of the aerodynamic spike, a wind tunnel program was designed to study the principle variables which affect the nozzle efficiency. These variables (Fig. 5) are: (1) primary jet discharge angle, (2) secondary-to-primary weight flow ratio, (3) centerbody expansion surface length, (4) nozzle expansion area ratio, and (5) primary chamber-to-ambient pressure ratio.

Throughout the study, one variable was systematically altered while the remaining were maintained constant. A simplified program was followed whereby those variables most influential on performance were separated and their study intensified. The highlights of the completed study are as follows.

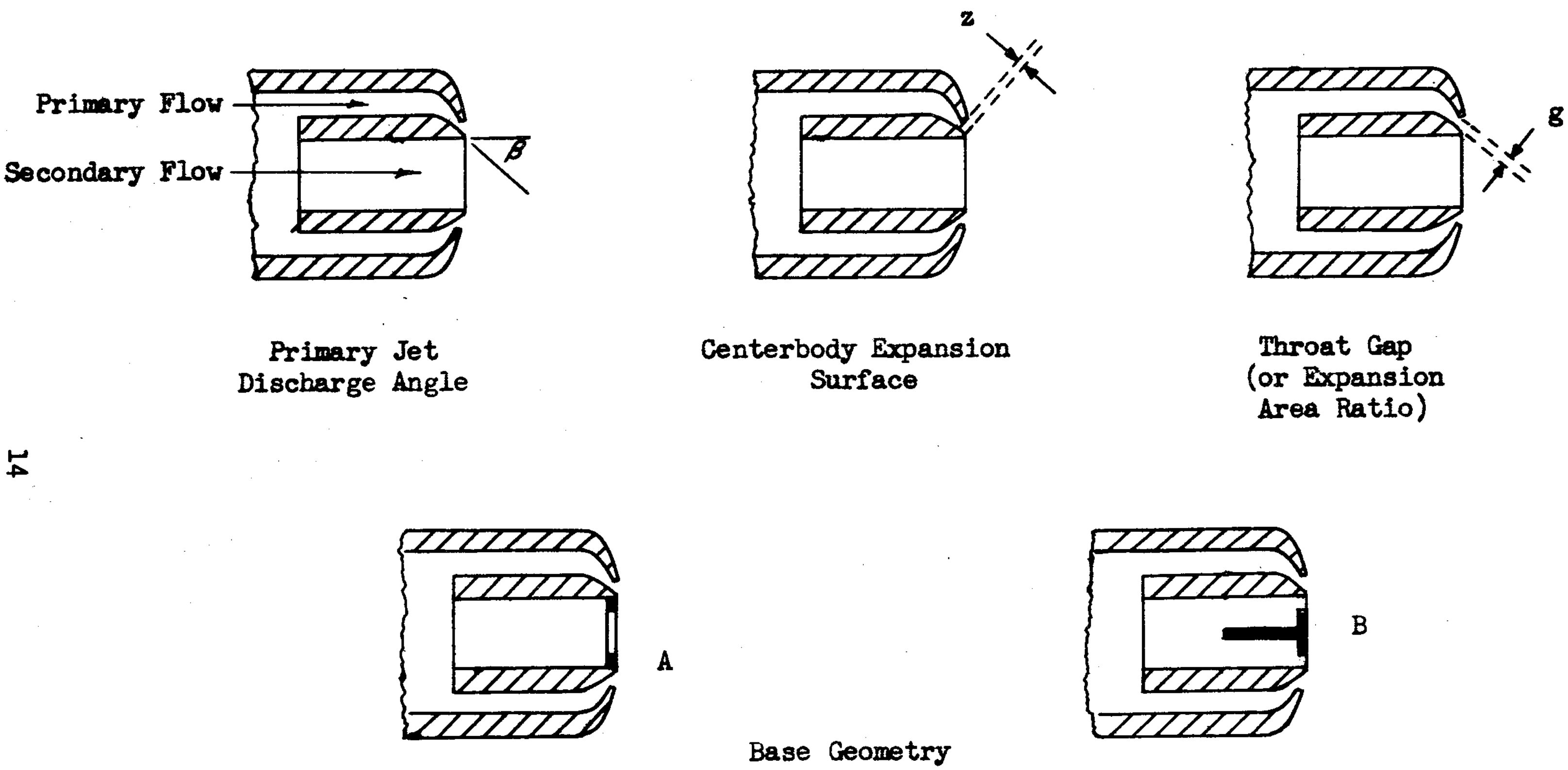

Fig. 5 . Geometric Variables Affecting Aerodynamic Spike Nozzle Performance

EFFECT OF PRIMARY JET DISCHARGE ANGLE - β

Four different primary jet discharge angles as indicated in Table 1 were examined. Figure 6 is an exploded view of one of the models used (β = 45 degrees). All models had approximately equal expansion area ratios and centerbody expansion surface length. These models were tested with no secondary flow to establish the effect of β on nozzle efficiency. Results of the study are indicated by Fig. 7. As shown in the figure, the nozzle efficiency is highest for primary discharge angles of 45 and 60 degrees. The efficiency of these two configurations is very similar throughout the pressure ratio range tested. The configuration with β equal to 30 degrees yielded efficiencies which were only a few percent lower than the efficiency of β's of 45 and 60 degrees, while the configuration with β equal to 15 degrees gave performance considerably lower. Slight geometric differences, especially in the centerbody expansion surface length, between the β's of 60, 45, and 30 degrees account for the slight difference in efficiencies between these configurations. However, the lower efficiency of the β of 15 degrees cannot be attributed to the slight geometric differences. This indicates efficiency is not very sensitive to changes in primary jet discharge angle β for relatively high values of this angle. A characteristic behavior of all of these configurations was to yield maximum performance at a pressure ratio which corresponds to design pressure ratio in a conical nozzle.

TABLE 1

AERODYNAMIC SPIKE NOZZLE

PRIMARY DISCHARGE ANGLE AND SECONDARY FLOW STUDY

$\epsilon \approx 25, \quad z/g \approx 3$

β, degrees	$\dot{W}_s$, percent of Primary
15	0
30	0, 1.27, 14.5
45	0, 1.8, 5.53, 10.10, 14.88
60	0, 1.67, 4.74, 10.06, 15.32

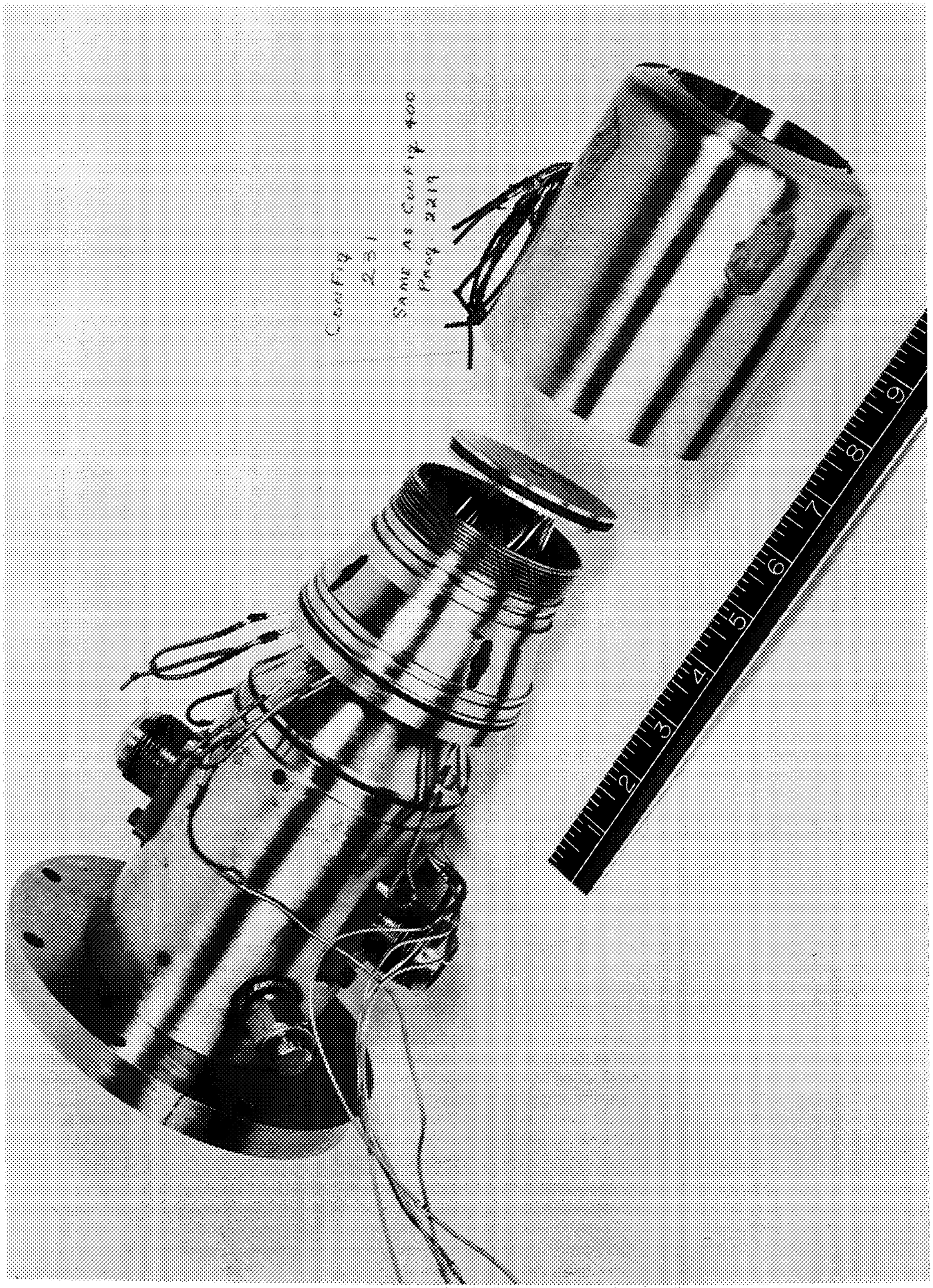

Fig. 6. Aerodynamic Spike Wind Tunnel Model, β equals 45 Degrees, Exploded View

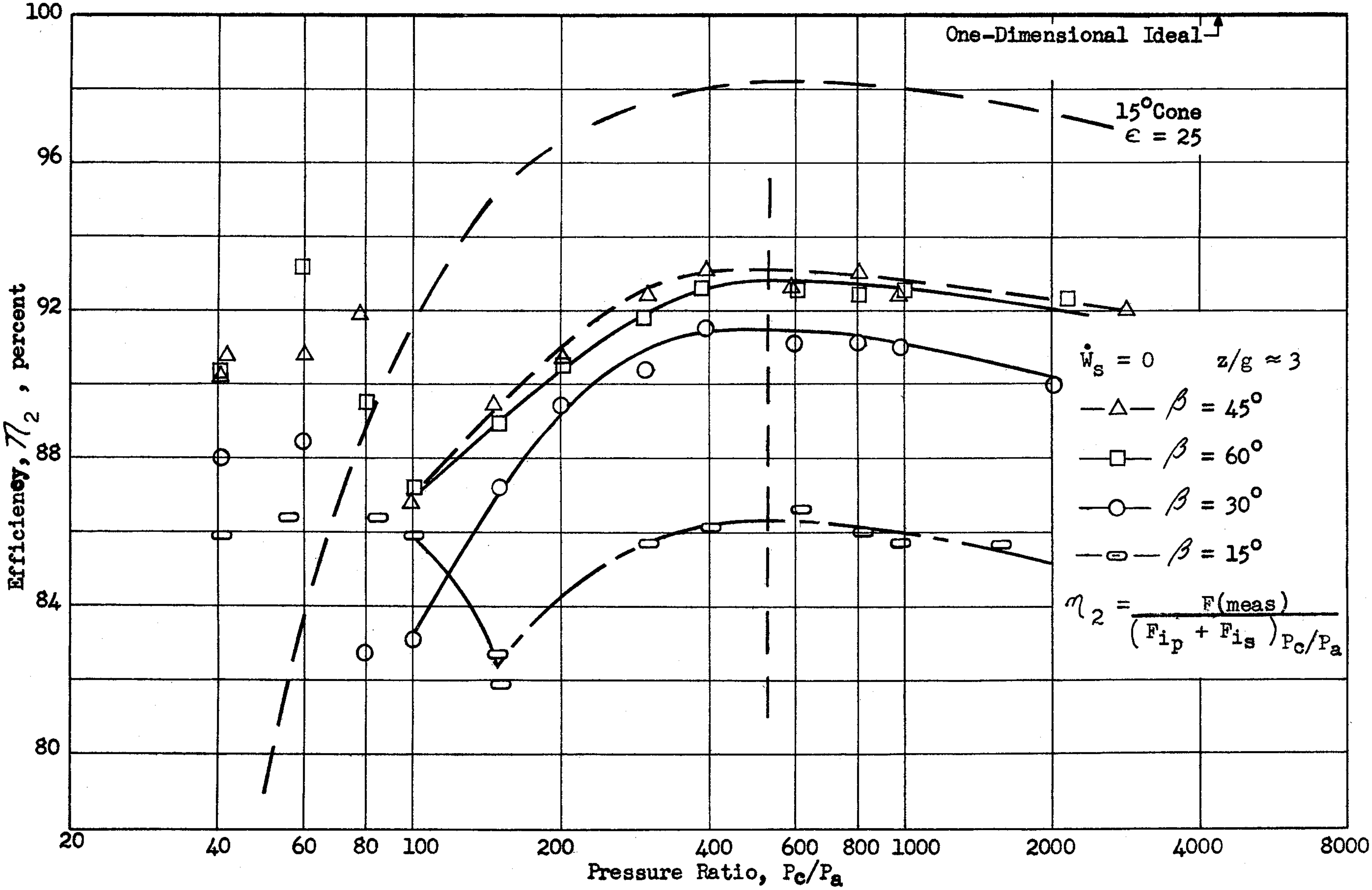

Figure 7. Aerodynamic Spike Nozzle Efficiency vs Pressure Ratio

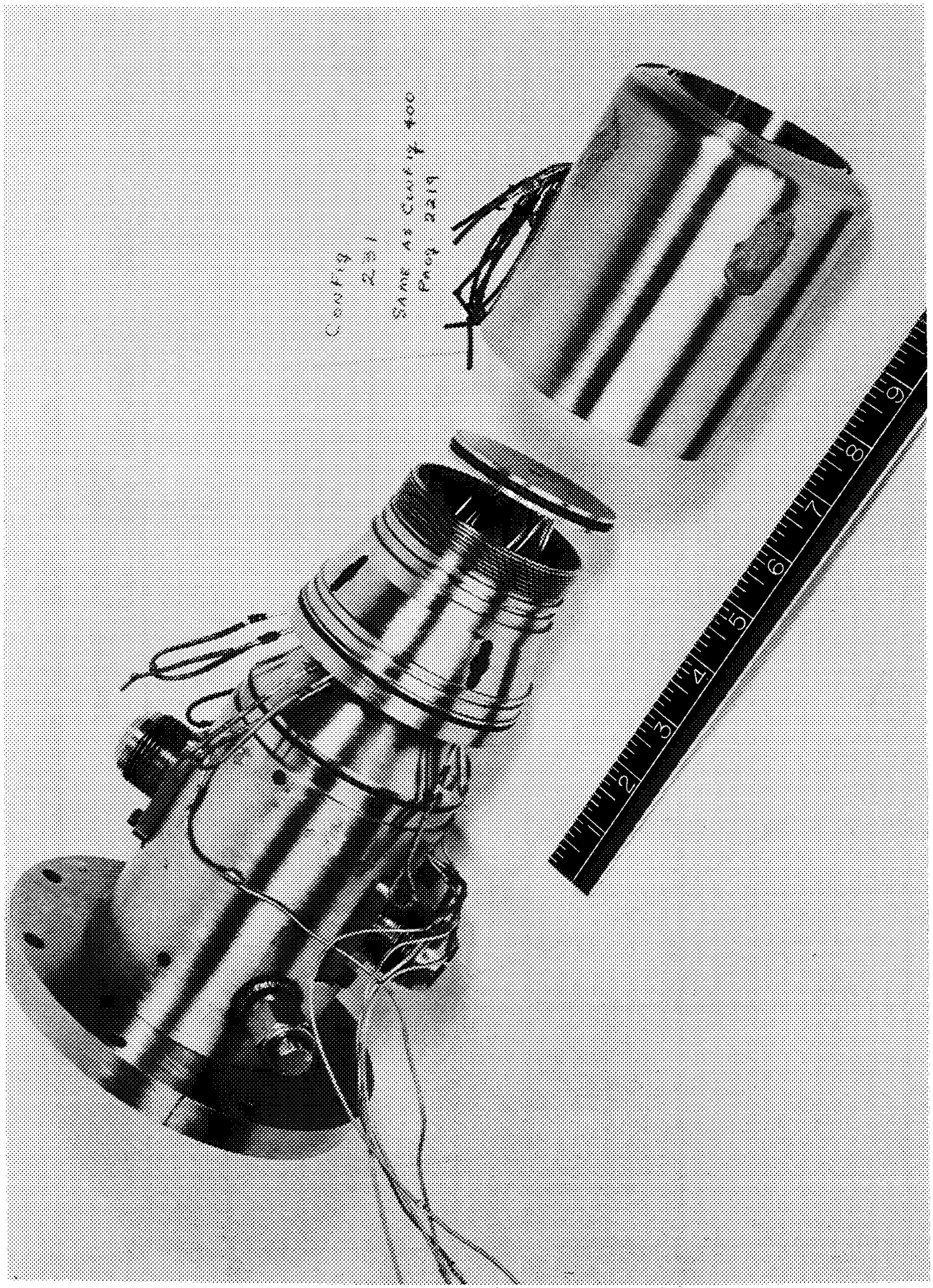

Fig. 6. Aerodynamic Spike Wind Tunnel Model, β equals 45 Degrees, Exploded View

12.7

* L represents nozzle wetted surface length for a 15-degree cone with equivalent expansion area ratio (i.e., Axial length ÷ cos 15-degrees).

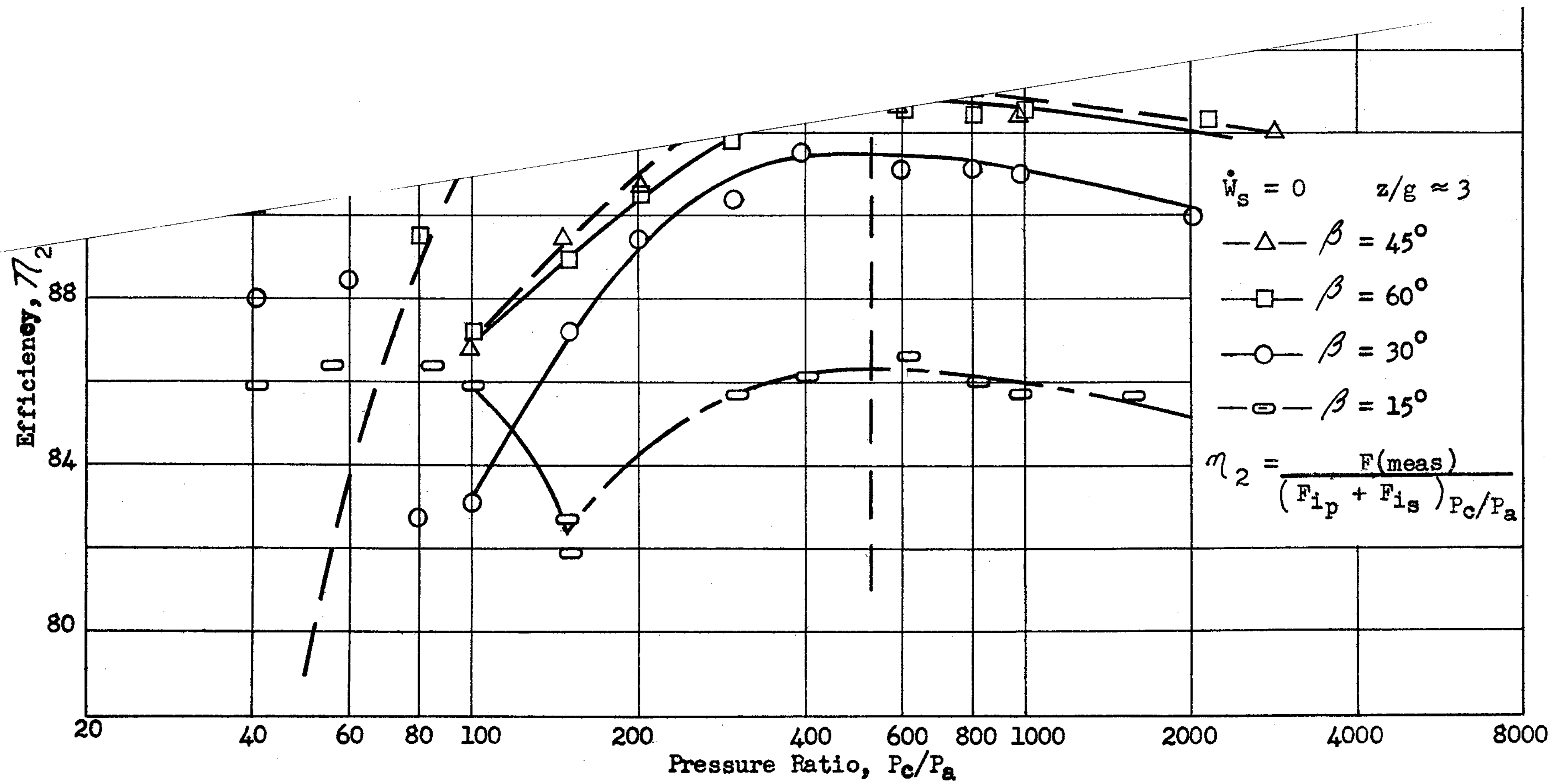

Figure 7. Aerodynamic Spike Nozzle Efficiency vs Pressure Ratio

ROCK
A DIVI

d

th

1.

TABLE 2

AERODYNAMIC SPIKE NOZZLE

CENTERBODY EXPANSION SURFACE STUDY

$\beta = 45^{\circ}\ 30'$, $\quad \dot{W}_s = 0\%\ \dot{W}_p$

z/ε	z/L, percent *	ϵ
0	0	27.21
3.10	2.31	22.16
6.71	4.23	24.10
12.7	7.97	25.43

* L represents nozzle wetted surface length for a 15-degree cone with equivalent expansion area ratio (i.e., Axial length ÷ cos 15-degrees).

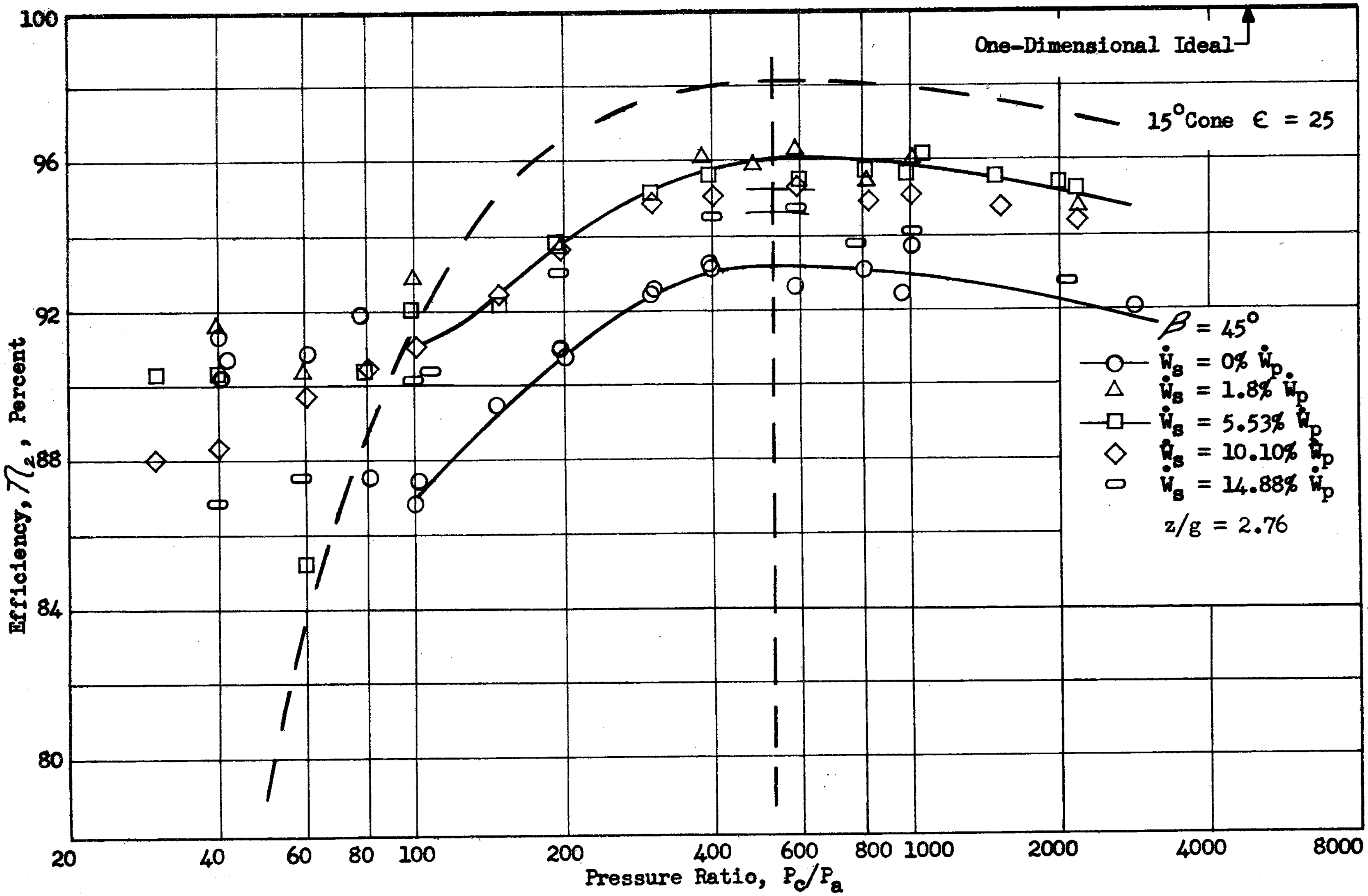

Figure 8 . Wind Tunnel Performance of Aerodynamic Spike Model.

TABLE 2

AERODYNAMIC SPIKE NOZZLE

CENTERBODY EXPANSION SURFACE STUDY

$\beta = 45^{\circ}\ 30'$, $\dot{W}_s = 0\%\ \dot{W}_p$

z/g	z/L, percent *	ϵ
0	0	27.21
3.10	2.31	22.16
6.71	4.23	24.10
12.7	7.97	25.43

* L represents nozzle wetted surface length for a 15-degree cone with equivalent expansion area ratio (i.e., Axial length ÷ cos 15-degrees).

ROCKETDYNE
A DIVISION OF NORTH AMERICAN AVIATION, INC

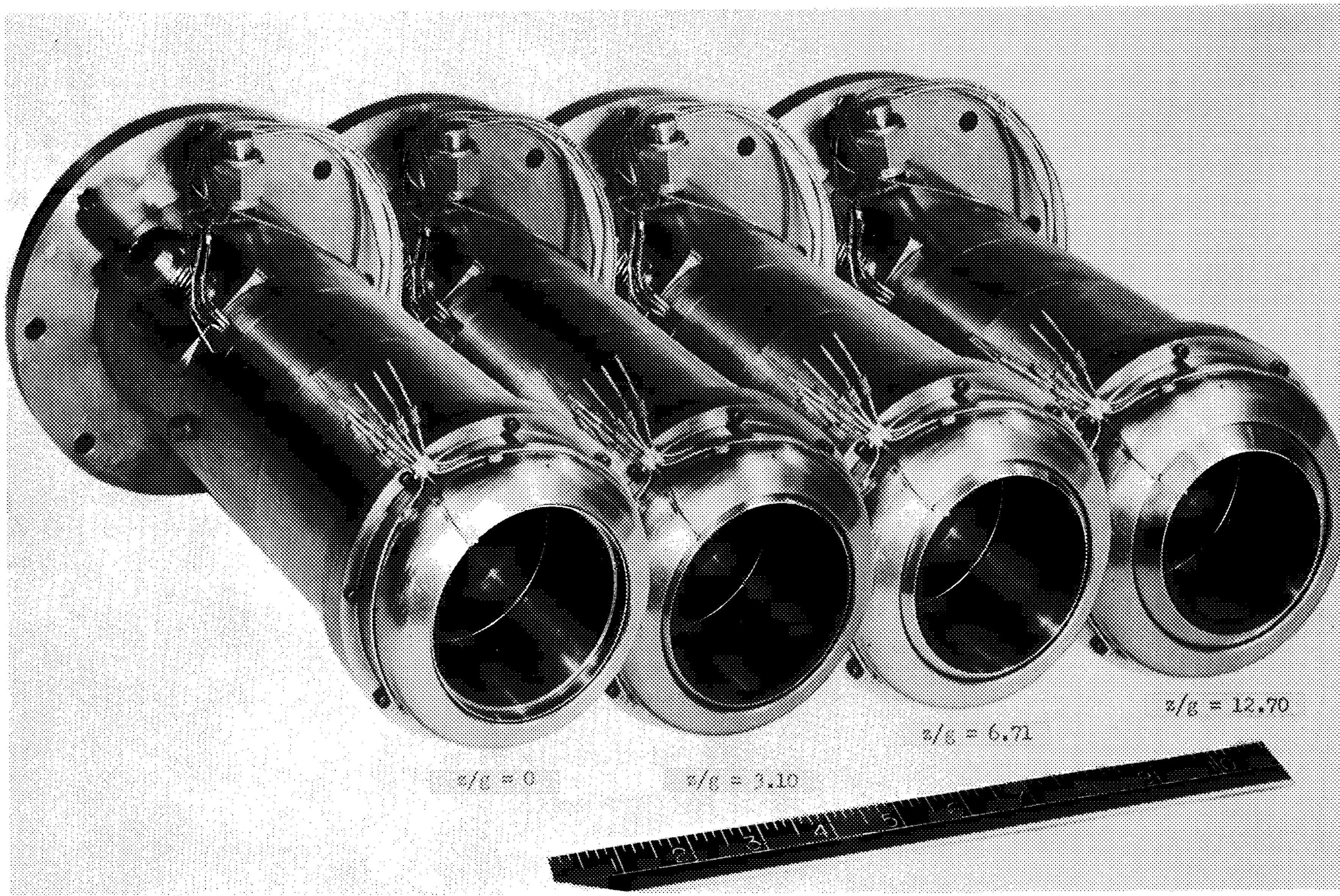

Fig. 9. Aerodynamic Spike Wind Tunnel Model, Adjustable z/g

CONFIDENTIAL

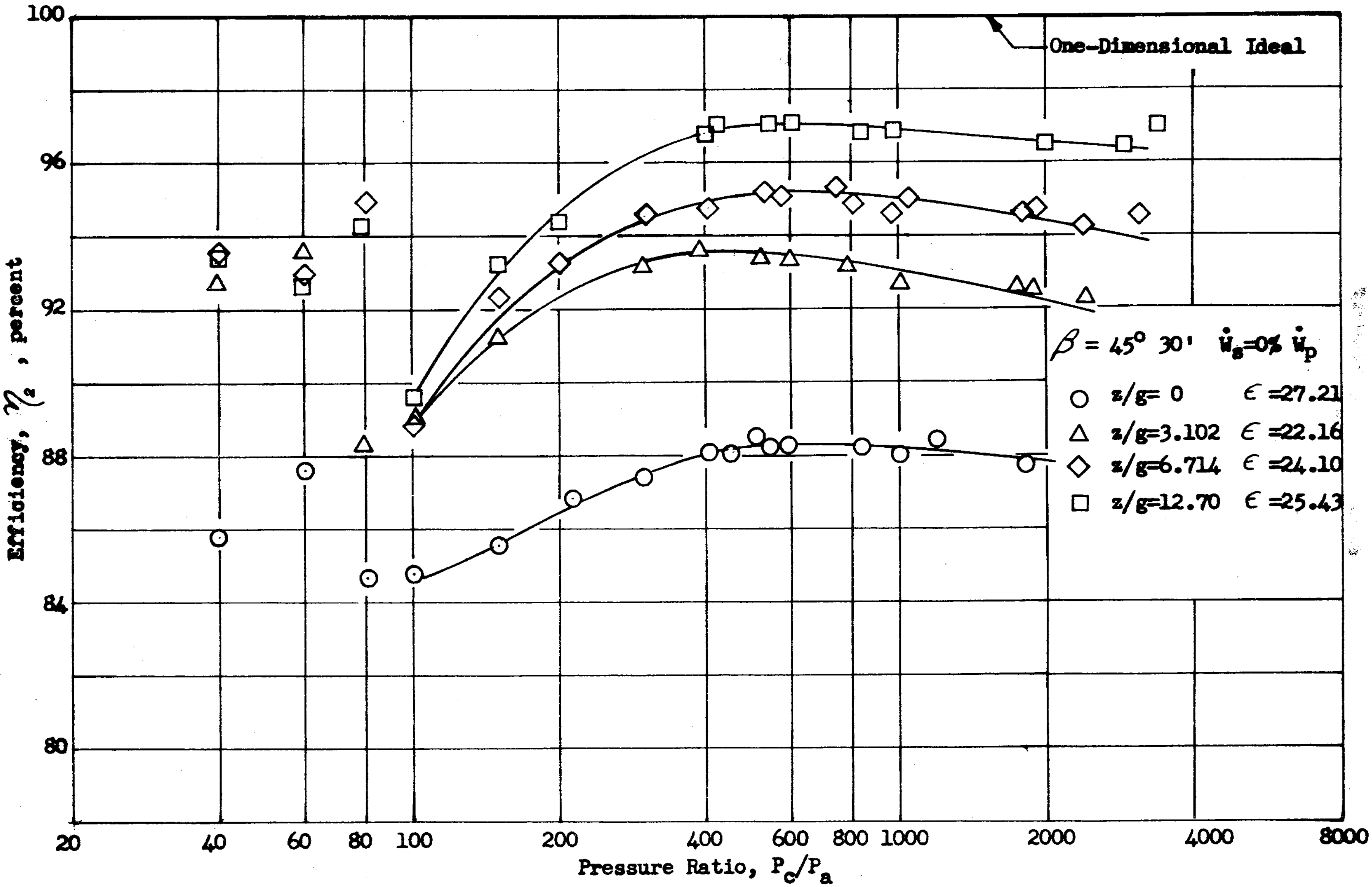

Fig. 10. Aerodynamic Spike Model Wind Tunnel Performance

further increase of 1.7 percent. The trends are for nozzle efficiency to increase with z/g; however, as z/g increases, the rate of gain in efficiency diminishes rapidly.

EFFECT OF EXPANSION AREA RATIO

One piece of information most important to the aerodynamic nozzle concept is the effect that expansion area ratio has on nozzle efficiency. Thrust developed by the nozzle depends on the aerodynamic boundary formed by the two streams. The nozzle geometric parameters which define expansion area ratio can affect this boundary and thus influence nozzle efficiency. Three area ratios as shown in Table 3 were evaluated in this study using no secondary flow. The wind tunnel models used in the study are depicted in Fig. 11. Results of the study in the form of efficiency versus pressure ratio curves appear in Fig. 12. All area ratios behaved in similar manners, i.e., their efficiencies had one maximum value at a pressure ratio which corresponds to design pressure ratio in a conical nozzle; their efficiency curves peaked at two different pressure ratios and contained a point of inflection located between the two peak values; and their efficiencies were considerably higher than sonic nozzle efficiencies.

For comprehensiveness of this interim report wind tunnel data on the aerodynamic nozzle configurations with expansion area ratios of 8 and 54 are included. Analysis of this data is continuing. During Phase II of the program the data will be made final.

TABLE 3

AERODYNAMIC SPIKE NOZZLE

EXPANSION AREA RATIO STUDY

$\beta = 45^{\circ}, 30', \quad z/g = 3, \quad \dot{W}_s = 0$

ϵ	z/g	z/L, percent *
8.14	3.38	8.43
22.16	3.10	2.31
53.89	3.71	1.03

* L represents nozzle wetted surface length for a 15-degree cone with equivalent expansion area ratio (i.e., Axial length ÷ cos 15-degrees).

~~CONFIDENTIAL~~

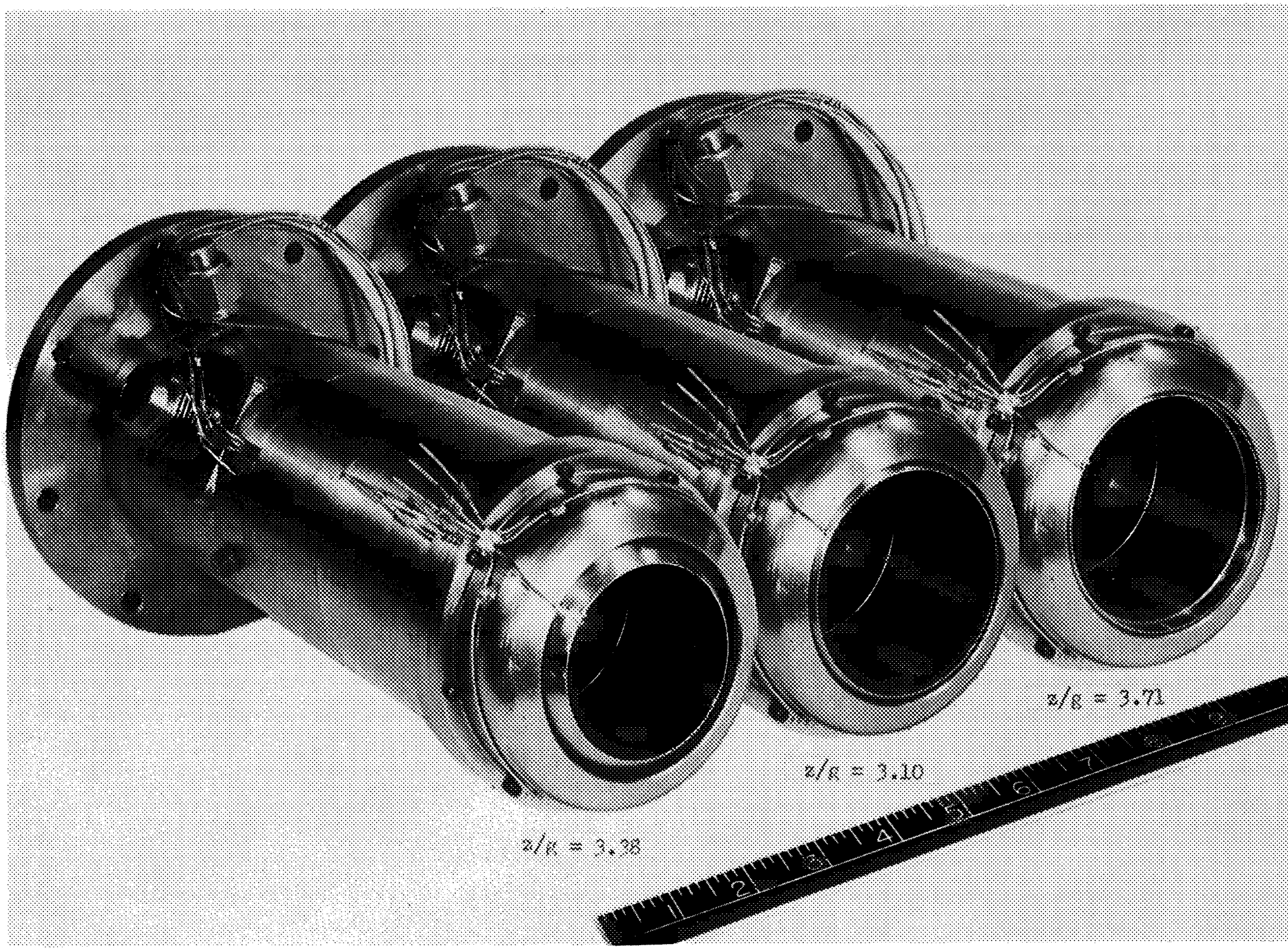

Fig. 11. Aerodynamic Spike Wind Tunnel Model, Adjustable ϵ

~~CONFIDENTIAL~~

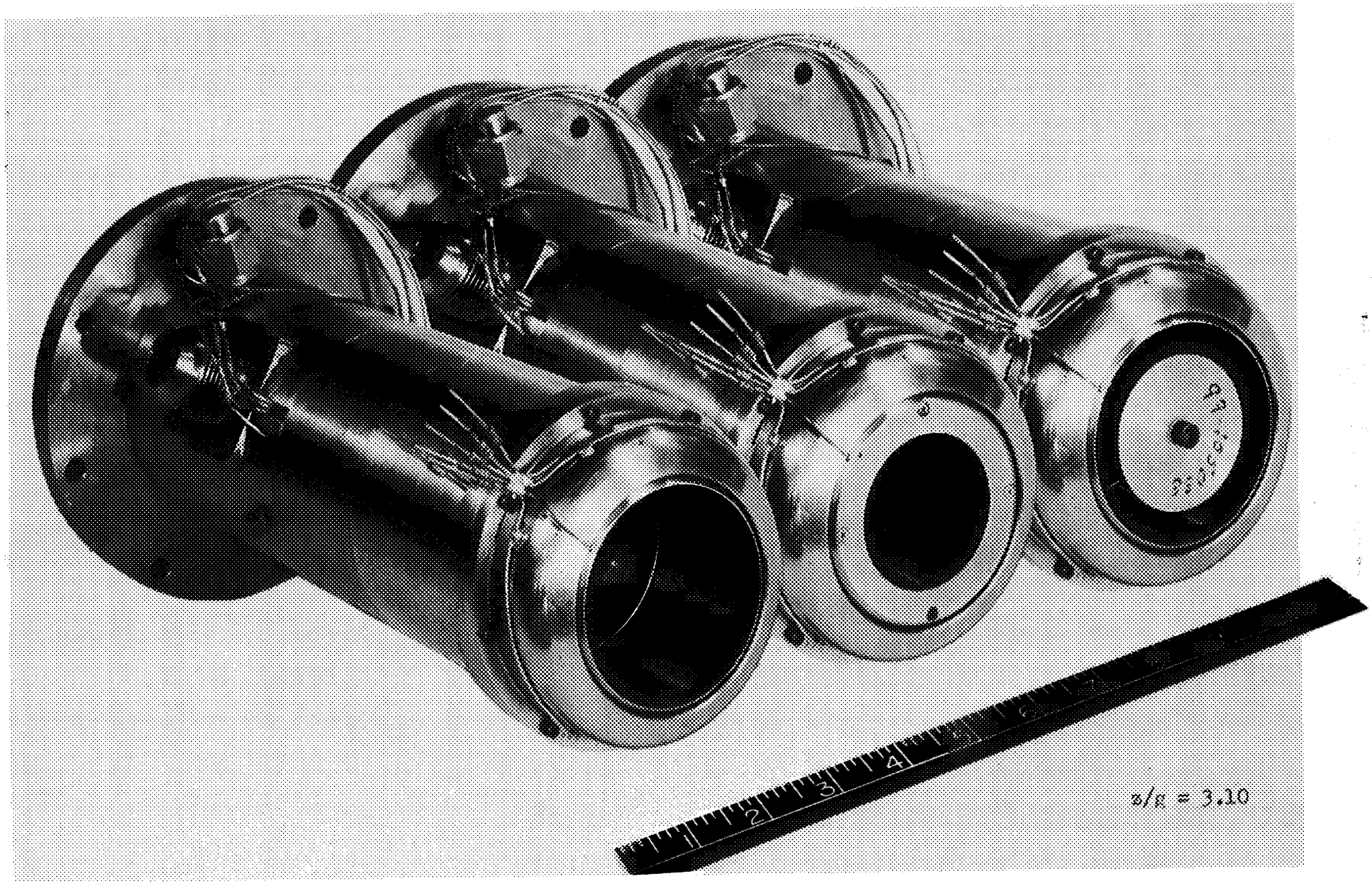

Fig. 13. Aerodynamic Spike Wind Tunnel Model, Adjustable Base Geometry

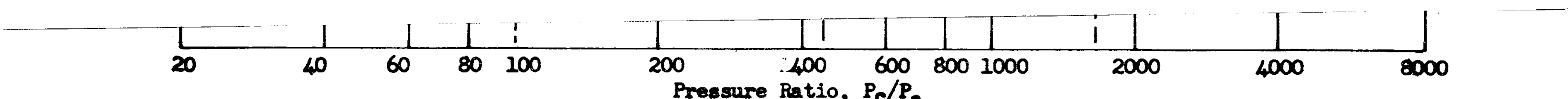

Fig. 12. Aerodynamic Spike Model Wind Tunnel Performance

BASE GEOMETRY STUDIES

The manner in which secondary gases are introduced into the region of interaction of primary and secondary flows depends to a large extent on the geometry of the base and may affect nozzle efficiency. The geometry of the base may vary considerably, depending on the placement of vehicle components such as propellant tanks, turbopumps, and hot gas ducts. Three configurations were evaluated in this study; one where the secondary passage is unobstructed, another where a peripheral portion of the secondary passage constituting 50 percent of the flow area is obstructed, and another where the central portion of the secondary passage constituting the same percentage is obstructed. The three configurations are depicted in Fig. 13 . Efficiencies of these configurations were determined at design pressure ratio. Both the configurations with peripheral and central blockage yielded the same efficiency. This efficiency was only a slight percent (0.3) lower than that of the configuration with no blockage.

SUMMARY OF COLD-FLOW STUDIES

For a comprehensive view of the wind tunnel program and to form general conclusions, the efficiency of all models at design pressure ratios were plotted versus the centerbody expansion surface length (z), for all primary jet discharge angles (β) and area ratios (ϵ). The plot

~~CONFIDENTIAL~~

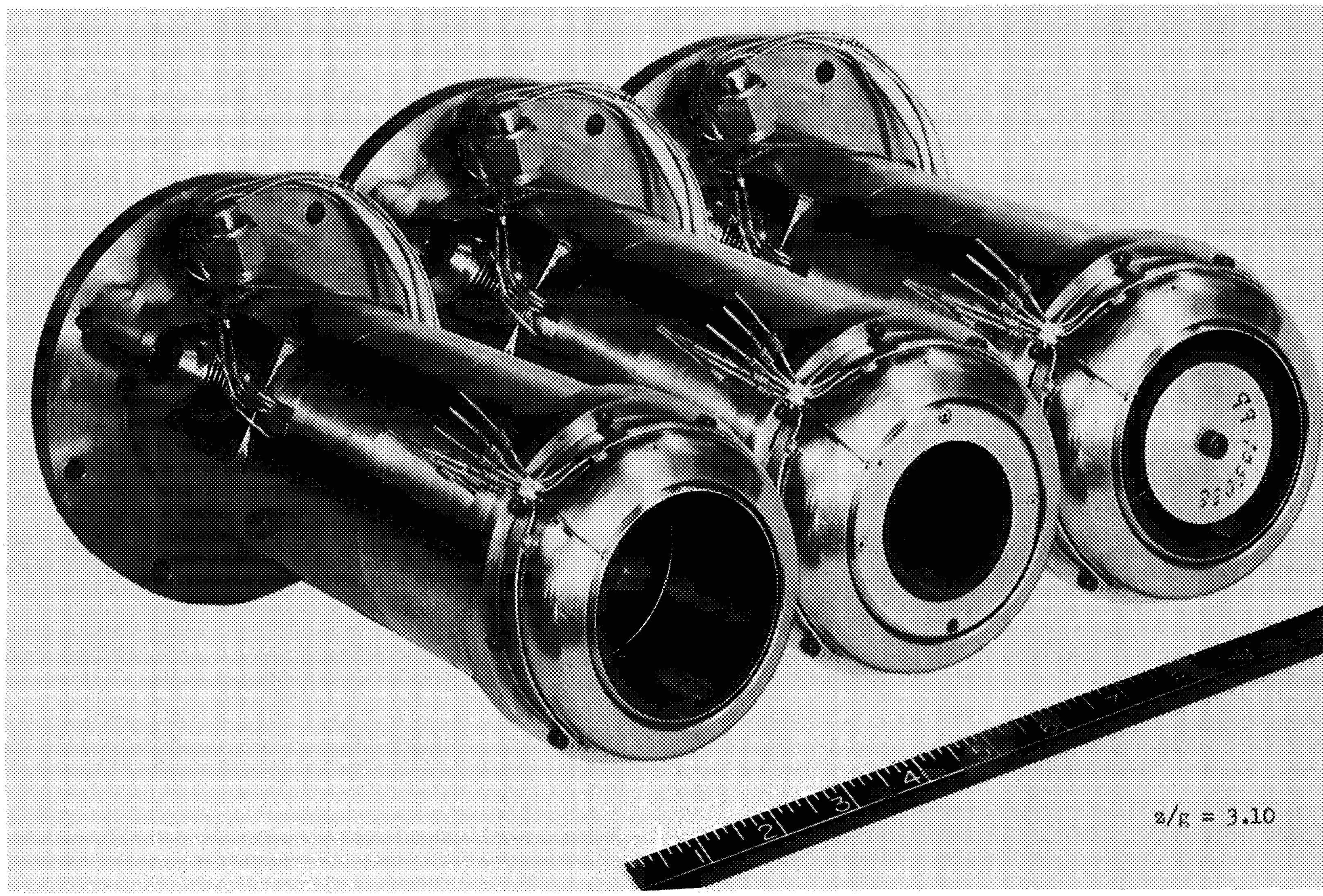

Fig. 13. Aerodynamic Spike Wind Tunnel Model, Adjustable Base Geometry

~~CONFIDENTIAL~~

was restricted to conditions of no secondary flow. Centerbody expansion surface length was expressed in terms of the nozzle wetted surface length (i.e., axial length ÷ cos 15-degrees) of a 15-degree cone with equivalent expansion area ratio. The data are shown in Fig. 14. A solid line was drawn through data points representing approximately equal expansion area ratios of 25 and β 's of 45 degrees.

The following observations may be made from the figure:

1. For all aerodynamic spike configurations tested with no secondary flow, efficiency is appreciably higher than sonic-nozzle efficiency.
2. With no secondary flow, some configurations exhibit performance comparable to conventional nozzle performance.
3. Data points for β 's of 60, 45 and 30 degrees follow the curve very closely; only when β equals 15 degrees is there a considerable deviation. This indicates that within a given range of β , efficiency is not critically affected by variations in β.
4. Efficiencies for β 's of 30, 60, and 45 degrees increase in that order. Their centerbody expansion surface also increase in that order: 1.33, 1.78, and 1.83. This indicates z is a critical parameter for all β 's within the given range.

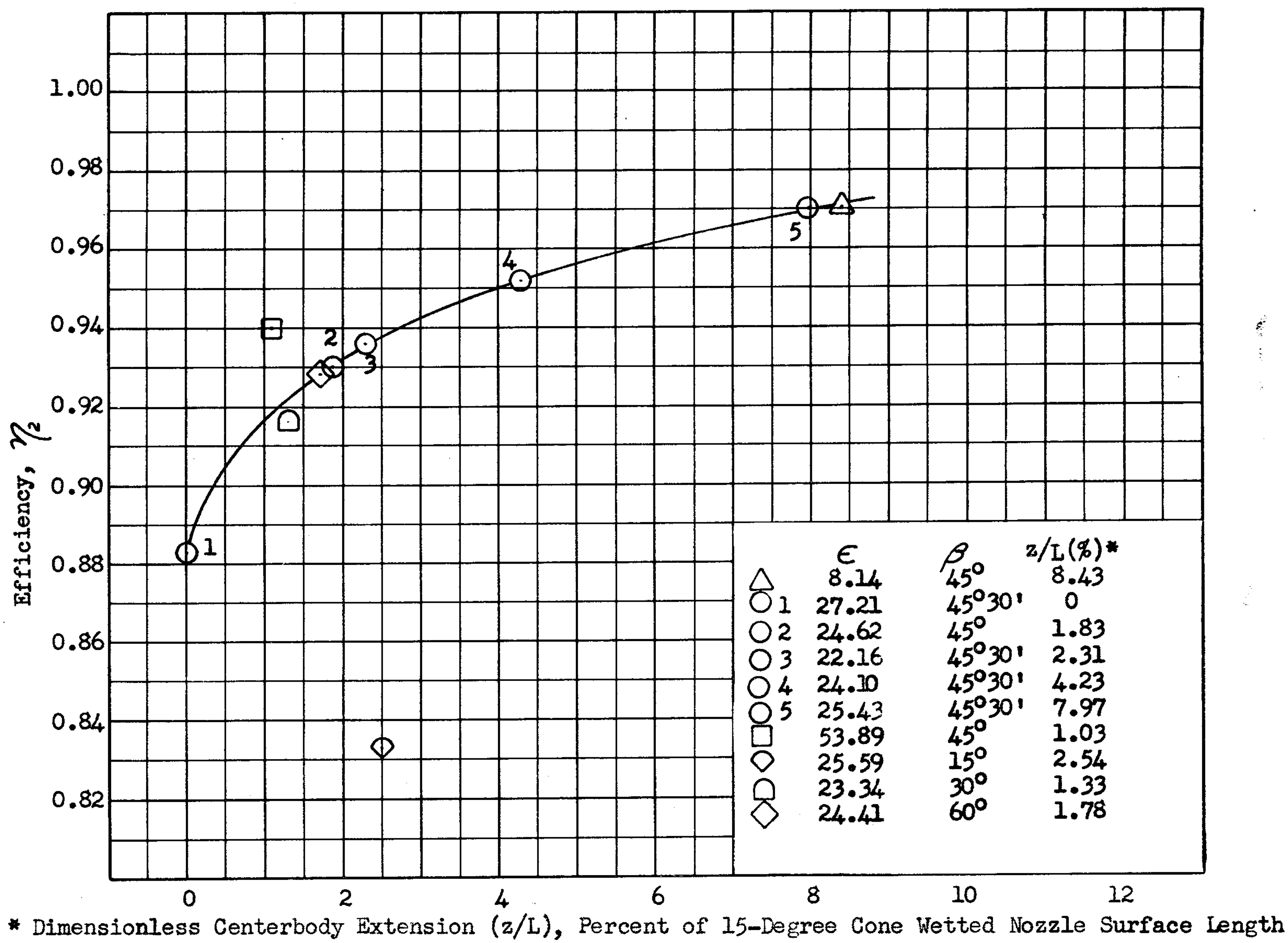

Fig. 14. Nozzle Efficiency η vs Centerbody Length (z, percent)
No Secondary Flow

5. Efficiencies for models with area ratios of 27.21, 22.16, 24.16, 25,43, increase sharply with z. The corresponding z's assume values of 0, 2.31, 4.23, and 7.97 percent.

6. Efficiency for the model with an area ratio of 8 and z of 8.45 percent also follows the curve, and is at the same high level as the efficiency of the model with an area ratio of 25.43 and z of 7.97 percent.

7. Efficiency for the area ratio of 53.89 and z of 1.03 percent does not follow the curve. Its low efficiency is, however, compatible with its low z.

Efficiency data obtained with the various configurations using several quantities of secondary flow are shown in Fig. 15 . Solid lines have been drawn through data points with equal β and ϵ . In Fig. 16 , the increase in efficiency over that with no secondary flow is plotted versus secondary flow for all configurations whose efficiency was presented in Fig. 15 . An average curve was drawn through all the points using data for configuration with β equal to 45 degrees and an ϵ of approximately 25 as a guide. The average curve indicates how the increase in nozzle efficiency decreases as $\dot{W}_s$ deviates from its most favorable value, and that appreciable gains in performance (in the order of 3 percent) may be obtained with secondary flowrates of approximately 5 percent of primary flow.

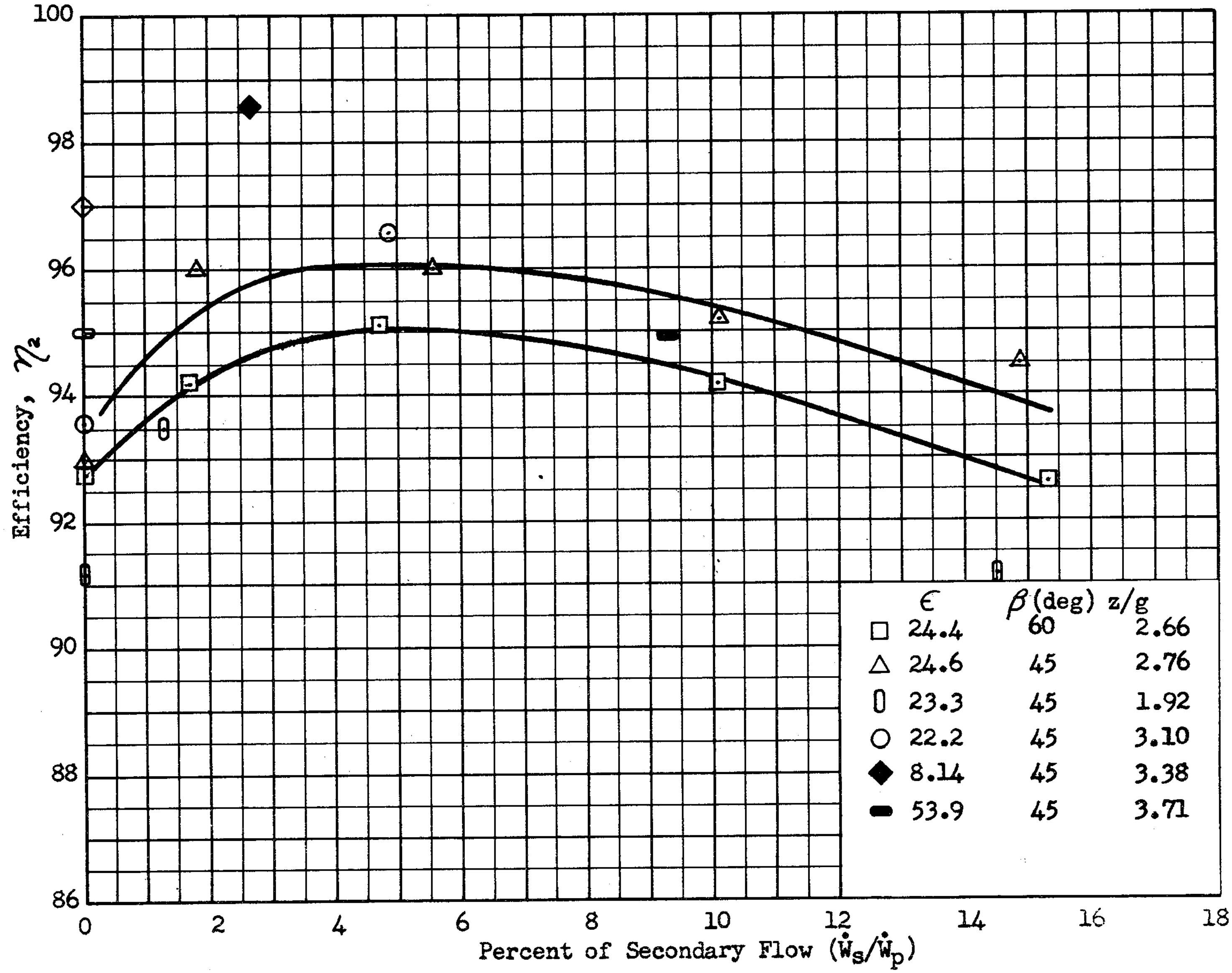

Fig. 15 . Effect of Secondary Flow on Aerodynamic Spike Nozzle Efficiency

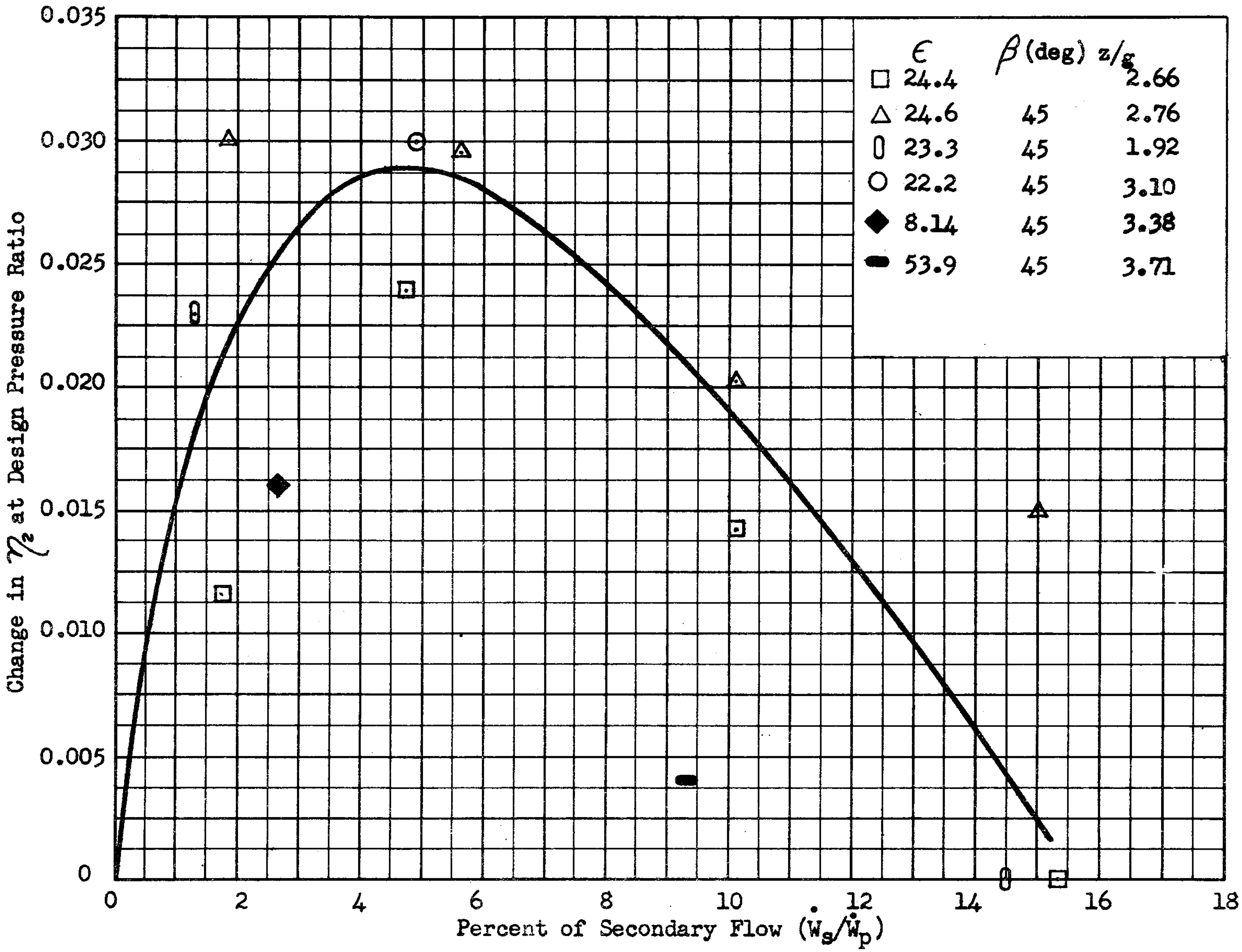

Fig. 16 . Effect of Secondary Flow on Aerodynamic Spike Performance

From these observations, the following general rules may be postulated for guidance in future work:

1. A slight variation in the z parameter produces a considerable effect in nozzle efficiency.

2. A slight variation in expansion area ratio ϵ does not produce appreciable changes in nozzle efficiency.

3. Appreciable variations in the primary jet discharge angles β do not produce substantial changes in the nozzle efficiency, as long as β is relatively high. It seems possible to have equally performing β's by selecting the proper z.

4. Given the proper z, efficiencies comparable to conventional nozzles may be achieved at all expansion area ratios investigated (ϵ = 8, 25, and 54).

5. The proper quantity of secondary flow always increases efficiency. For the configurations tested so far this quantity was 5 percent of primary flow. However, the quantity of secondary flow could vary substantially with z.

HOT-FIRING STUDY - AERODYNAMIC SPIKE

General objectives of these studies were to demonstrate the hot-firing feasibility of the aerodynamic spike nozzle and to derive hot-firing data for correlation with cold flow data. The model was designed after the best performing configuration evaluated in the initial phase of the wind tunnel program. For simplicity uncooled copper walls were employed in the nozzle. Already existing gas generator and main chamber injector hardware were utilized. The model developed a maximum thrust of 7000 pounds utilizing liquid oxygen and kerosene propellants for both the primary and secondary flows. Secondary flowrates ranging from 0 to 10 percent of the primary flows were used. Design mixture ratio in the primary gases had a value of 2.1 while the secondary gases had a mixture ratio value near 0.35. The model installed at the test complex is depicted in Fig. 17; base pressure instrumentation may be seen inside the base cavity, chamber pressure instrumentation and fuel entrance port are located around the outer nozzle wall.

The specific objectives of the hot-firing program were (1) to demonstrate the hot-firing feasibility of the aerodynamic spike configuration, (2) to demonstrate similar behavior of cold-flow and hot-firing models by showing the same general appearance of the flow field, the same base pressure trends, and the same tendency of base pressures to be higher than ambient,

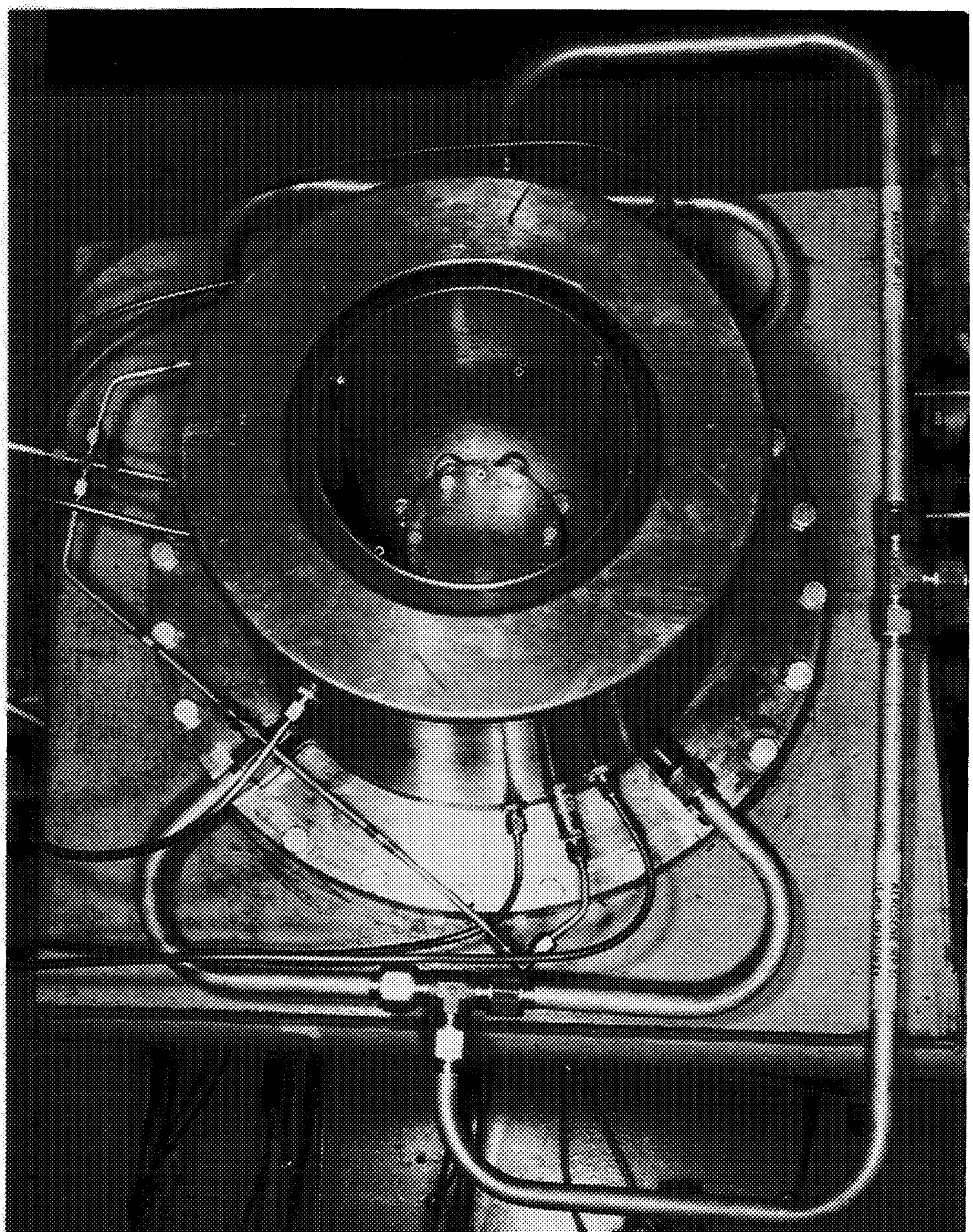

Fig. 17 Aerodynamic Spike Hot-Firing Model

and (3) to demonstrate similarity in performance of cold-flow and hot-firing models by showing higher-than-sonic nozzle performance with no secondary flow and an increase in nozzle efficiency with secondary flows.

NATURE OF FLOW FIELD

Twelve hot-firing tests were made, of which eight furnished enough information to satisfy all the specific objectives named above. By motion picture closeups of the exhaust jet it was evident that the flow fields of cold-flow and hot-firing models were similar. This may be seen by comparing Fig. 18, an enlarged frame of the hot-firing motion picture, with Fig. 19, a Schlieren photograph of the exhaust jet in the wind tunnel model.

BASE PRESSURES

Behavior of base pressure was similar with both models as may be seen in Table 4. The base pressure parameter shown in the table normalizes chamber pressure, throat area, and base area differences between the two models. With both models closure of the primary jet occurred as pressure ratio was increased. After closure of the primary jet constant base pressures were recorded with both models. These base pressures were higher than ambient in both cases. However, the pressure ratio at which constant base pressure occurred was different for the two models

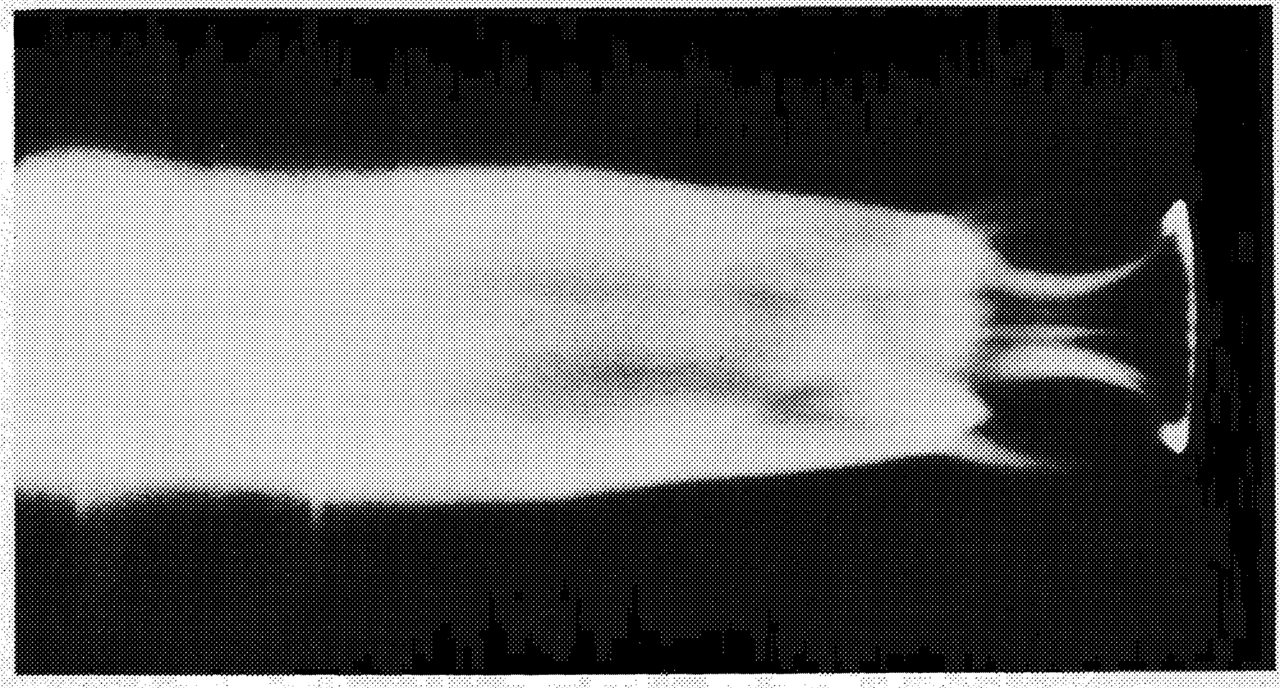

Fig. 18. Aerodynamic Spike Hot-Firing Exhaust Jet

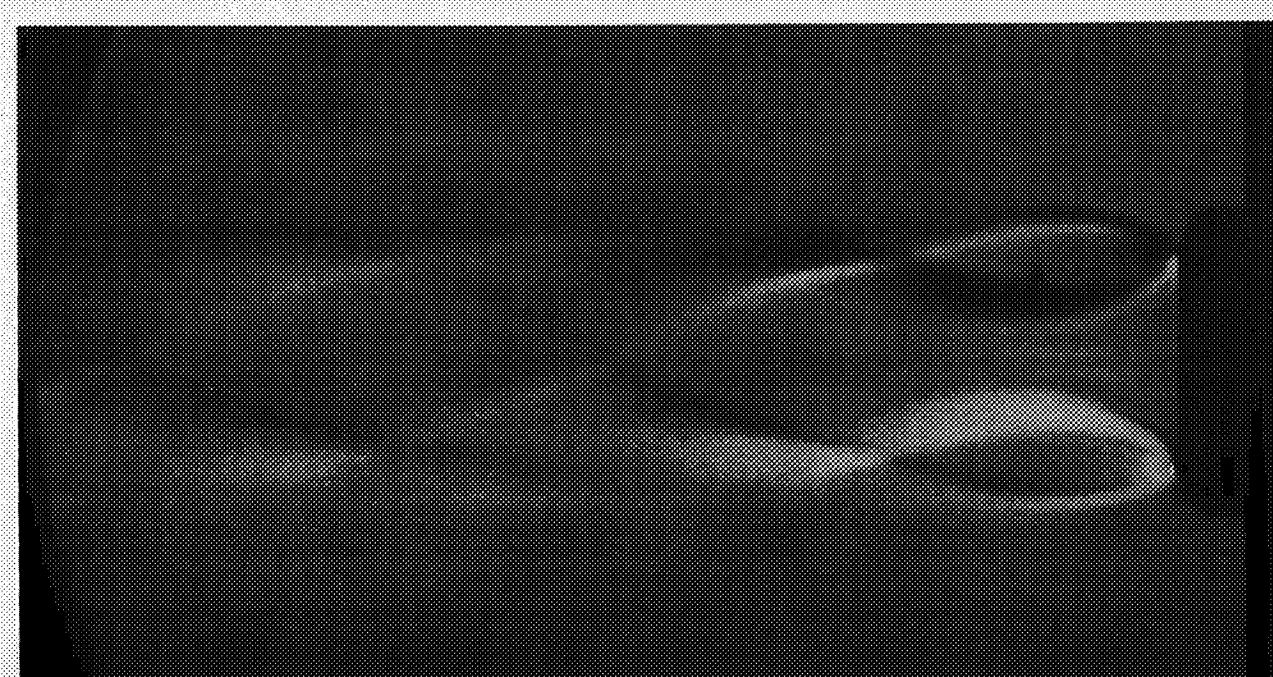

Fig. 19. Aerodynamic Spike Cold-Flow Exhaust Jet

TABLE 4

TEST RESULTS, BASE PRESSURES

Test No.	P_c psia	P. R.	A_t sq.in.	$\bar{P}_B$ psia	W (1) Weight Flow Parameter, percent	ϕ_H (2) Base Pressure Parameter Hot-Firing	ϕ_C (3) Base Pressure Parameter Cold-Flow	(4)
3048	316.4	23.10	-	-	-	-	-	
3049	313.2	22.90	-	-	-	-	-	
3050	351.7	25.70	8.471	-	-	-	-	
3051	347.4	25.40	8.471	16.85	0	0.270	0.202	(31)
3052	419.7	30.70	8.615	20.86	0	0.272	0.202	(38)
3053	361.4	26.40	8.614	20.62	1.97	0.312	0.274	(38)
3054	365.0	26.65	8.670	22.31	3.29	0.331	-	
3055	427.7	31.20	8.726	24.16	1.74	0.305	-	
3056	528	38.60	8.726	32.56	5.26	0.333	-	

Notes:

(1) $W = \frac{\dot{W}_s \sqrt{(RT)_s}}{\dot{W} \sqrt{(RT)_p}}$ (2) $\phi_H = \frac{P_B A_B}{P_c A_t}$ (3) $\phi_C = \frac{P_B A_B}{P_c A_t}$

(4) Pressure ratio corresponding to cold-flow base pressure parameter is shown in parenthesis.

due to the difference in specific heat ratio of the cold-flow and hot-firing gases. The effect on base pressure of increasing secondary flow is to increase base pressures, for both models.

NOZZLE EFFICIENCY

The nozzle efficiencies realized with the hot-firing aerodynamic spike model employing primary gases (specific heat ratio $\gamma = 1.235$) only are shown in Fig. 20. Also included in the figure are efficiencies of the cold-flow model employing primary gas only, and efficiencies of a sonic nozzle, both nozzles using gas with $\gamma = 1.4$. Hot-firing and cold-flow nozzle efficiencies are considerably higher than those of the sonic nozzle. Efficiencies increase with pressure ratio for both models. This is not the case for the sonic nozzle. As a result of the difference in specific heat ratio between cold-flow and hot-firing the efficiency curves are displaced in the efficiency-pressure-ratio plane, and peaks in the curves will occur at different design pressure ratios.

Nozzle efficiencies (η_o) with secondary flow are shown in Table 5. The subscript (o) indicates the secondary gas is not accounted for in the calculations, for comparison with cases where secondary flow is obtained from sources outside the nozzle; the subscript (1) indicates secondary gases are accounted for but expanded to atmospheric pressure from the pressure prevailing in the base, for comparison with conventional thrust chamber

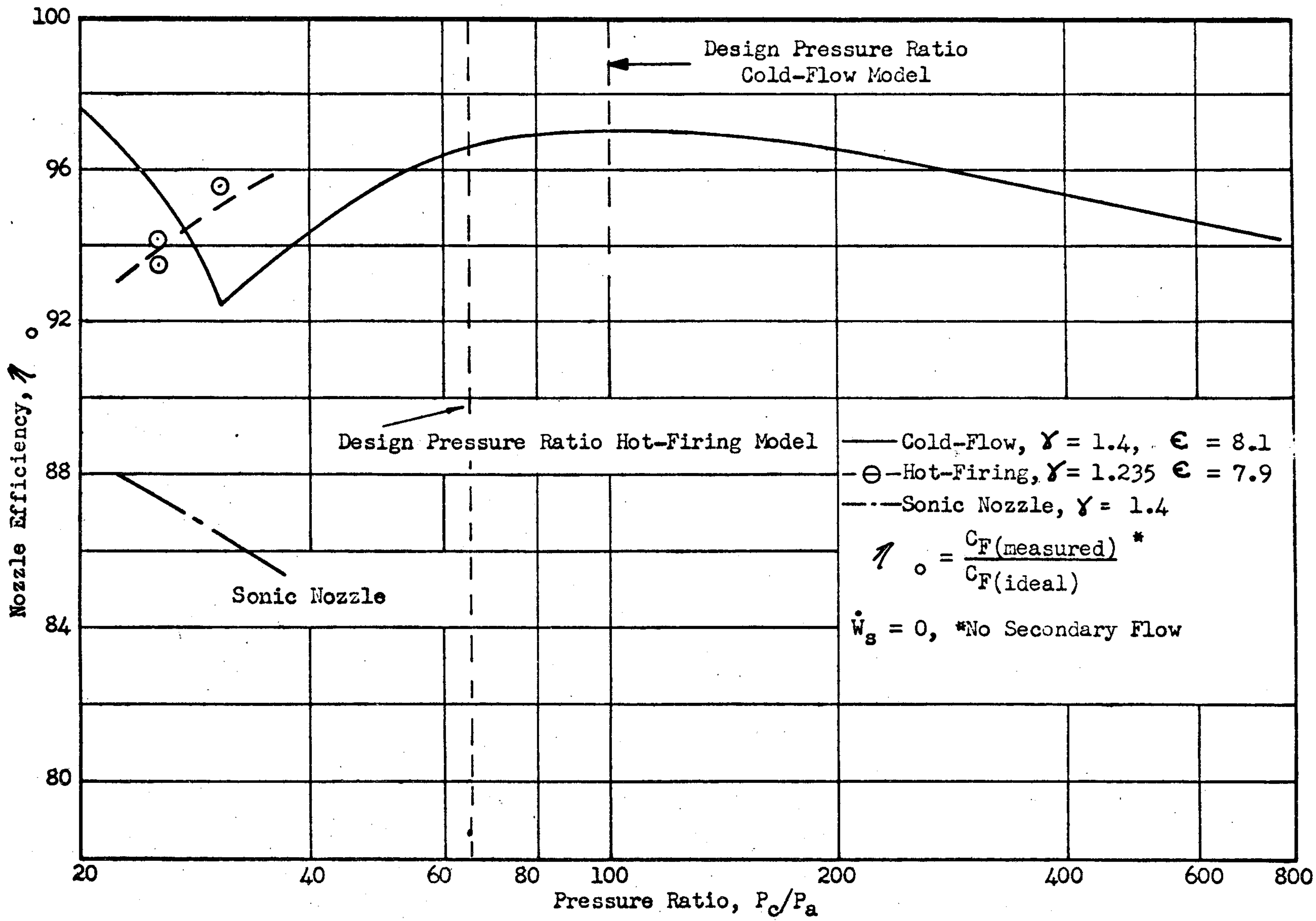

Fig. 20 . Hot-Firing and Cold Flow Aero-Spike Nozzle Efficiencies, $\dot{W}_s = 0$

TABLE 5

AERODYNAMIC SPIKE NOZZLE

HOT-FIRING DATA

Test No.	P. R.	W	$I_s=\left(\frac{F}{\dot{W}_p+\dot{W}_s}\right)$	$\eta_{c_p^*}$	η_0	η_1	η_2
3050	25.7	0	201.4	0.83	0.935	0.935	0.935
3051	25.4	0	200.4	0.82	0.942	0.942	0.942
3052	30.7	0	210.2	0.83	0.956	0.956	0.956
3053	26.4	0.0197	198.5	0.85	0.953	0.942	0.925
3054	26.7	0.0329	199.1	0.87	0.967	0.959	0.928
3055	31.2	0.0174	203.7	0.85	0.954	0.942	0.928
3056	38.6	0.0526	247.7	0.97	1.010	0.981	0.975

efficiencies; the subscript (2) indicates secondary flows are accounted for and assumed available for expansion at the same pressure as the primary gases, for comparison of efficiencies with conventional engines. The second column (η_1) indicates thrust chamber or nozzle efficiency increases with an increase in secondary flow.

Also indicated in the table are specific impulse values (including secondary flows) and characteristic velocity efficiencies realized in the test program.

WIND TUNNEL STUDIES - CONCENTRIC TUBE AERODYNAMIC NOZZLE

The objectives of the wind-tunnel studies on the concentric tube aerodynamic nozzle were to supplement available cold-flow data through tests of shorter nozzle length-to-primary-diameter ratios (L/D), and to derive cold-flow data for correlation with hot-firing data. Hardware used in this study was obtained from a previous program. Length-to-diameter ratios were selected based on previous results. Two nozzle expansion area ratios (ϵ) were tested with various length-to-diameter ratios (L/D) and secondary-to-primary weight flow ratios ($\dot{W}_s/\dot{W}_p$) as shown in Table 6 . Analysis of data obtained indicated that for a given expansion area ratio, (1) there exists an optimum pressure ratio which closely corresponds to design pressure ratio for a 15-degree cone with equivalent expansion area ratio, (2) a length-to-diameter ratio exists for which a maximum efficiency is realized, and (3) a secondary-to-primary weight flowrate exists for which a maximum efficiency is obtained at design pressure ratio.

The above results may be ascertained by inspection of Figs. 21 through 23 . Figure 21 is a plot of nozzle efficiency with the best L/D and $\dot{W}_s/\dot{W}_p$ tested for nozzles with expansion area ratio of 5.6 and 22.4. Both nozzles exhibit a peak in their efficiencies at a pressure ratio which corresponds to design pressure ratio of the corresponding conical nozzle. A slight decrease in nozzle efficiency with area ratio is evident from the figure.

TABLE 6

COLD-FLOW TESTS

AERODYNAMIC NOZZLE - CONCENTRIC TUBES

	$\frac{L}{D_p}$	$\frac{L}{D_p}$ (% Conic)	$\frac{\dot{W}_s}{\dot{W}_p}$	P.R.	No. Tests
5	0	0	0	40-1000	36
	0.70	30	.054*		
	1.20	52	.17		
	1.64*	71*			
22	2.0	28.5	0	40-1000	36
	2.9*	41.5*	.113*		
	5.5	79.0	.23		

* Best Conditions

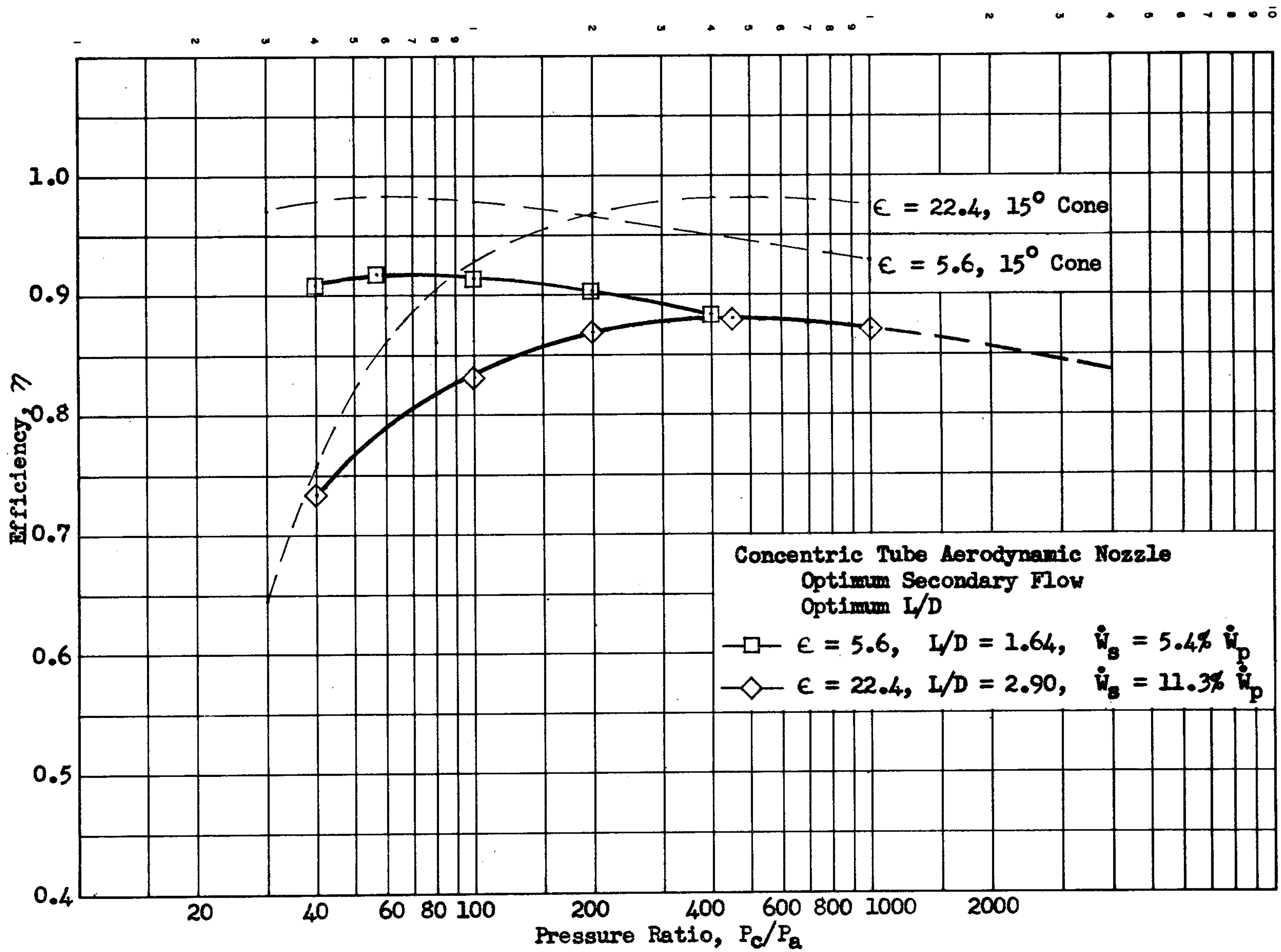

Figure 21 . Performance Trend with Pressure Ratio

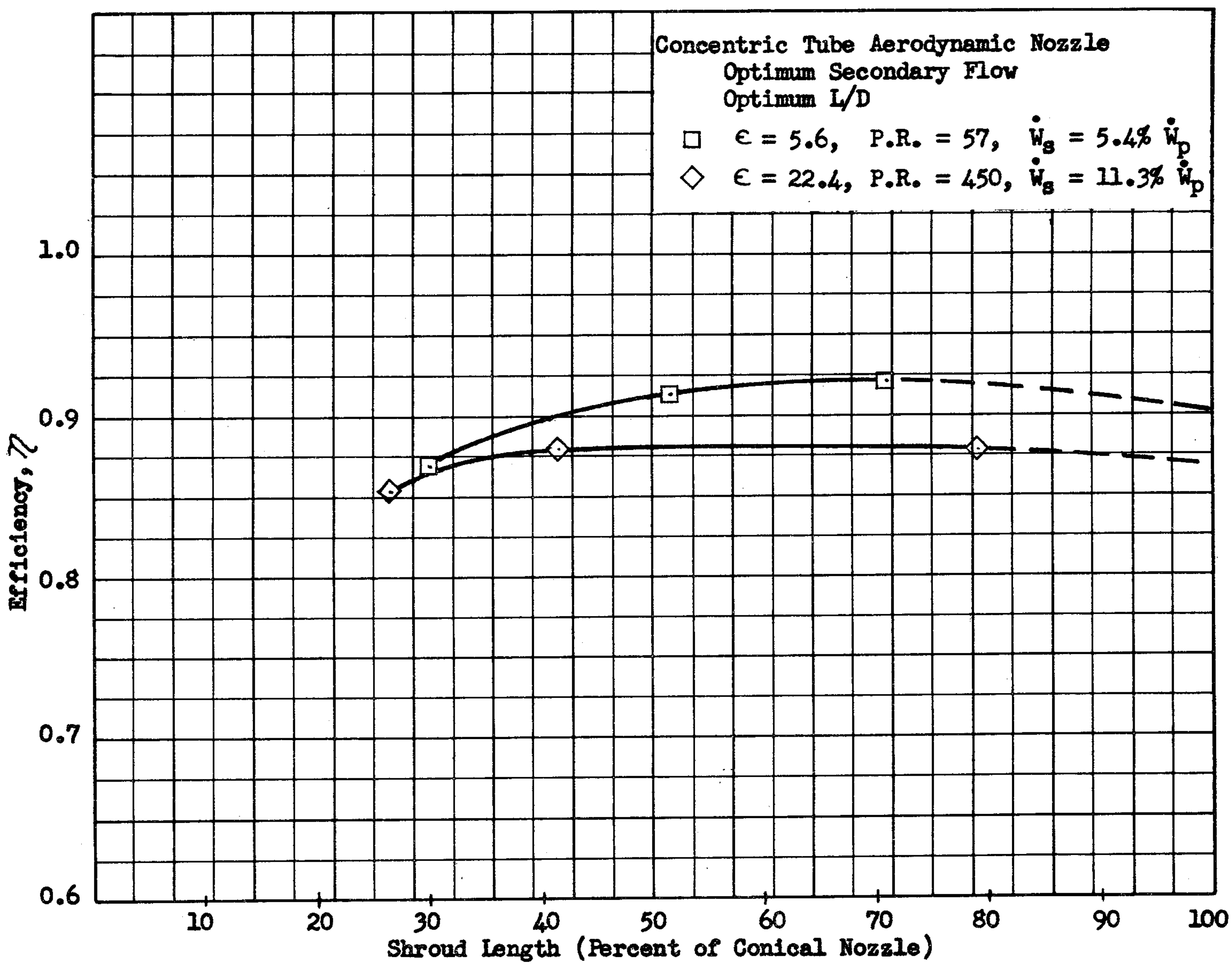

Figure 22 . Effect of Shroud Length on Efficiency

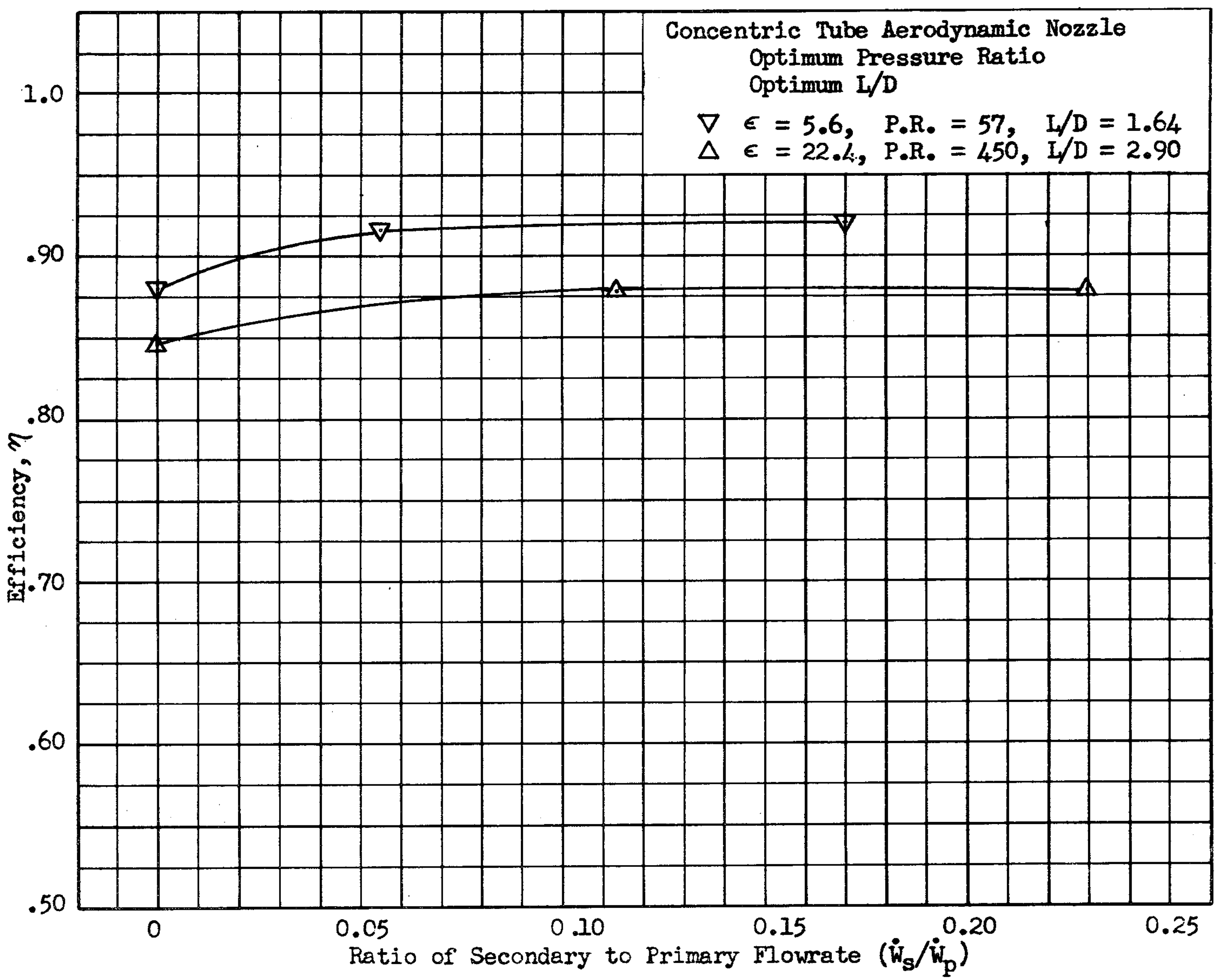

Figure 23. Effect of Secondary Flow on Efficiency

The effect of nozzle length on efficiency is shown in Fig. 22 where efficiencies plotted are those obtained at design pressure ratio with the secondary flowrate of best performance. The length of the nozzle is expressed in terms of the length of a 15-degree cone. Curves for the two nozzles indicate an optimum nozzle length exists.

The effect of secondary flow on efficiency is shown in Fig. 23 . Nozzle efficiency in this case was obtained at the pressure ratio and length-to-diameter ratio of best performance. Both expansion area ratios indicate an optimum secondary flowrate exists.

HOT-FIRING STUDY - CONCENTRIC TUBE AERODYNAMIC NOZZLE

A hot-firing model of the concentric tube aerodynamic nozzle, available from a previous program, was tested in this study. The model utilized a Vernier engine LOX-kerosene injector, a concentric tube nozzle configuration with $L/D = 1.6$ and $\epsilon = 5.6$, and various quantities of gaseous nitrogen in the secondary. The nozzle efficiencies are plotted versus pressure ratio in Fig. 24 for the various quantities of secondary flow used. It is seen that nozzle efficiency increases with secondary flow. Cold-flow efficiency data for the corresponding wind tunnel model is also shown in Fig. 24 . Satisfactory correlation was obtained, although there still are deviations due to differences in specific heat ratio between cold-flow and hot-firing gases.

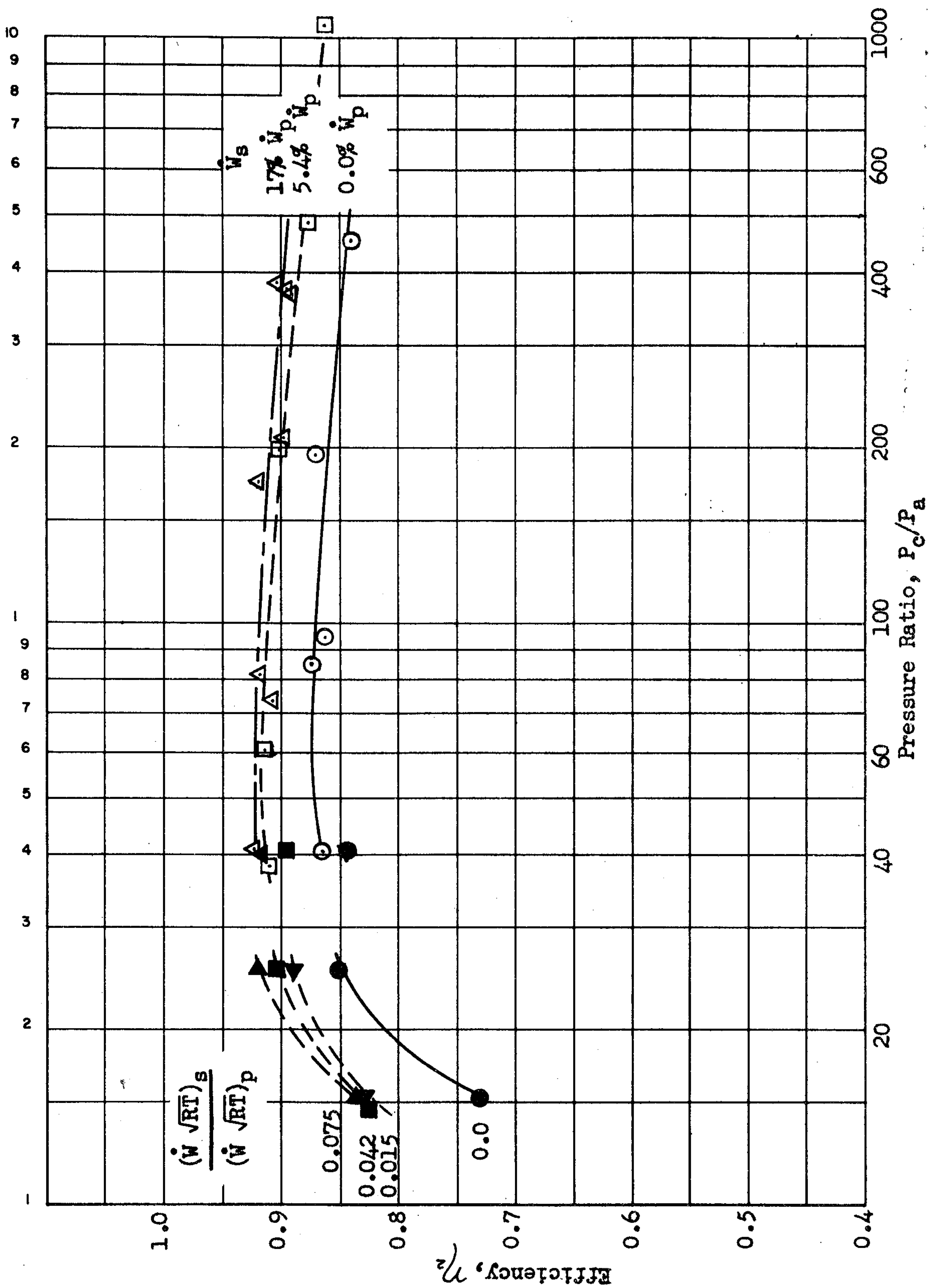

Fig. 24. Efficiency vs Pressure Ratio, Concentric Tube Aerodynamic Nozzle